Theory of directed polymers

Randall D. Kamien, Pierre Le Doussal,* and David R. Nelson
Lyman Laboratory of Physics, Harvard University, Cambridge, Massachusetts 02138
(Received 20 December 1991)

We develop a theory of polymers in a nematic solvent by exploiting an analogy with two-dimensional quantum bosons at zero temperature. We argue that the theory should also describe nematic polymers in an *isotropic* solvent. The dense phase is analyzed in a Bogoliubov-like approximation, which assumes a broken symmetry in the phase of the boson order parameter. We find a stiffening of the longitudinal fluctuations of the nematic field, calculate the density-density correlation function, and extend the analysis to the case of ferro- and electrorheological fluids. The boson formalism is used to derive a simple hydrodynamic theory which is indistinguishable from the corresponding theory of nematic polymers in an isotropic solvent at long wavelengths. We also use hydrodynamics to discuss the physical meaning of the boson order parameter. A renormalization-group treatment in the dilute limit shows that logarithmic corrections to polymer wandering, predicted by de Gennes, are unaffected by interpolymer interactions. A continuously variable Flory exponent appears for polymers embedded in a *two*-dimensional nematic solvent. We include free polymer ends and hairpin configurations in the theory and show that hairpins are described by an Ising-like symmetry-breaking term in the boson field theory.

PACS number(s): 36.20.Ey, 05.40.+j

I. INTRODUCTION

A. Overview

The statistical mechanics of directed, interacting lines has received renewed attention recently. This problem is, for example, directly relevant to the behavior of high-T_c superconductors in a magnetic field [1,2]. In these systems, above a critical external field H_{c1}, the magnetic field penetrates the material in the form of lines, each carrying one quantum of magnetic flux. The flux lines can be viewed as "polymers" aligned with the direction of the external field up to thermal fluctuations. Due to their mutual repulsion, these lines can form various states such as a triangular solid [3] or isotropic and hexatic entangled fluids [1,4]. Glassy states are also possible, induced either by local disorder [5,6] or simply by very long disentanglement relaxation times [1,7]. Detailed calculations for flux liquids are possible by exploiting a mapping onto the statistical mechanics of boson world lines in two spatial and one timelike dimension [1].

Many other physical systems consist of extended one-dimensional objects aligned in one direction [8,9,10]. Stiff biological macromolecules such as DNA [11], helical synthetic polypeptides such as poly(γ-benzyl glutamate) (PBG) [12,13], discotic liquid crystals composed of stacks of disk-shaped molecules [14,15], and micelles of amphiphilic molecules [16] can all form crystalline columnar phases with in-plane order, as well as nematic phases with fluidlike in-plane order. Although stiffer chains align more easily, some nematic polymer liquid crystals can also be formed with chains of relatively low rigidity, by alternating a nematogenic unit with a flexible hydrocarbon spacer [17–19]. The transition from isotropic melt to nematic is achieved experimentally by lowering the temperature [20] or more frequently by increasing the concentration. Steric repulsion is sufficient to produce alignment at high enough concentration, although many other interactions can be present depending on the material: Van der Waals attraction, electrostatic forces [21,22], hydration forces, etc. Ferrofluids [23] and electrorheological fluids [24] are also composed of chains of particles, in this case aligned by external magnetic or electric fields.

In a recent paper [25], Ao, Wen, and Meyer have presented x-ray scattering data on PBG that is in many ways strikingly similar to predictions [1] for neutron diffraction by flux lines. These authors stress an analogy between polymer configurations and a fictitious "dynamics" of two-dimensional particles moving along the direction of alignment and show that the distinctive "bow-tie" scattering contours change character in the limit of small momentum transfers.

There are, however, significant differences between these directed polymerlike objects and flux lines. Although oriented nematic polymers in a solvent wander along a preferred axis, just as thermally excited flux lines do, the average polymer direction represents a spontaneous, rather than externally imposed, broken symmetry. Even if the monomer chains are aligned by an external electric or magnetic field, the lines are typically of variable length and need not span the system, unlike flux lines. Nematic polymers can, moreover, make relatively low-energy hairpin turns, because of the symmetry of the director field under $\mathbf{n}\rightarrow-\mathbf{n}$. Such "backtracking" can usually be ignored for flux lines [1,2].

In a recent paper [26] two of us adapted methods developed for flux lines to these systems, taking the above differences into account. We showed that the boson field theory of Ref. [1] becomes applicable to directed polymer melts upon adding a source term, in analogy with the des Cloiseaux method for isotropic polymer solutions. The

spontaneously broken symmetry of nematic polymers requires, in addition, coupling the boson order parameter to a massless fluctuating background director field.

In this work, we describe these calculations in detail and discuss as well their validity in the dilute limit. Calculations for dilute directed polymers are a straightforward extension of results for flux lines [1] in the case of electrorheological and ferrofluids. The dilute limit is more interesting, however, when the average polymer direction represents a spontaneously broken symmetry. Nematic polymers in an isotropic solvent will, of course, eventually crumple into an isotropic phase upon dilution [27]. An analysis of the transition to an isotropic polymer melt would take us beyond the scope of this paper. We shall, however, consider a dilute collection of polymers aligned by a solvent which is itself a short-chain nematic fluid. As pointed out by de Gennes [8], the Goldstone modes associated with the nematic solvent already lead to logarithmic anomalies in the wandering of one isolated polymer. Additional logarithms appear when interactions are included, and a full renormalization-group analysis is required to sort out the details. Yet another complication appears when we allow for *hairpins* in the polymers as they meander through the nematic solvent. The polymers are now crumpled on scales large compared to the hairpin spacing. We find in this case that an Ising-like symmetry-breaking term appears in the boson field theory.

Table I contains a summary of the different types of directed polymeric systems considered in this paper. Note that flux lines in high-temperature superconductors are the simplest case, because (1) they contain no free ends and (2) hairpins are highly disfavored by the external magnetic field. Although hairpins are disfavored by the magnetic and electric fields necessary to produce aligned chains in ferro- and electrorheological fluids, free ends are, of course, unavoidable. The behavior of nematic polymers and polymers in a nematic solvent is complicated both by the existence of free ends and hairpins, and because the alignment can be produced by a "soft" broken symmetry instead of an external field.

We consider here only *Gaussian* fluctuations about the state that describes directed polymer melts in the dense hydrodynamic limit. While this paper was in preparation, we learned of interesting work by Toner [28] who introduces nonlinearities directly into the hydrodynamic theory of nematic polymers. Toner concludes that these nonlinear terms eventually trigger a breakdown of hydrodynamics (i.e., a singular dependence of hydrodynamic parameters on a wave vector) at sufficiently long wavelengths. It would be interesting to see if such a breakdown also occurred in the more microscopic boson theory developed here.

TABLE I. Characteristics of the different physical systems considered in this paper.

System	Mechanism for alignment	Free ends important?	Hairpins important?
Nematic polymers	Spontaneously broken symmetry	Yes	Yes
Polymers in a nematic solvent	Induced by solvent	Yes	Yes
Ferro- and electrorheological fluids	External fields	Yes	No
Flux lines in high-temperature superconductors	External field	No	No

B. Model

We shall concentrate on nematic polymers, regarded as directed polymers interacting with a background nematic field. By imposing a magnetic field H, or taking the limit of very large Frank constants, we can, if desired, recover results for directed polymer melts with an externally imposed direction. We start with a nematic free energy

$$F_n=\frac{1}{2}\int d^2r_\perp \int dx\,[K_1(\nabla_\perp\cdot\delta\vec{\mathbf{n}})^2+K_2(\nabla_\perp\times\delta\vec{\mathbf{n}})^2 +K_3(\partial_z\delta\vec{\mathbf{n}})^2+H(\delta\vec{\mathbf{n}})^2]\,, \tag{1.1}$$

where the $\{K_i\}$ are the usual Frank constants for splay, twist, and bend, and $\delta\vec{\mathbf{n}}(\vec{\mathbf{r}})=(\delta n_x(\vec{\mathbf{r}}_\perp,z),\delta n_y(\vec{\mathbf{r}}_\perp,z))$ is a vector representing a small deviation of director field $\mathbf{n}(\mathbf{r})$ from its average orientation along the z axis, $\mathbf{n}(\mathbf{r})\approx(\delta\vec{\mathbf{n}},1)$. We neglect for now polymer free ends and hairpin turns and describe the position of the ith polymer as it traverses the nematic medium by a function $\mathbf{R}_j(z)=(\vec{\mathbf{r}}_j(z),z)$. The N polymer lines interact with each other and the nematic field via a free energy adapted from Ref. [8]

$$F_p=\frac{1}{2}\kappa\sum_{j=1}^{N}\int dz\left[\frac{d^2\vec{\mathbf{r}}_j}{dz^2}\right]^2 +\frac{1}{2}g\sum_{j=1}^{N}\int dz\left[\frac{d\vec{\mathbf{r}}_j}{dz}-\delta\vec{\mathbf{n}}(\vec{\mathbf{r}}_j(z),z)\right]^2 +\frac{1}{2}\sum_{\substack{i,j=1\\ i\neq j}}^{N}\int dz\,V(|\vec{\mathbf{r}}_i(z)-\vec{\mathbf{r}}_j(z)|)\,. \tag{1.2}$$

Here κ is the polymer bending rigidity, while g controls the coupling between the local polymer direction and the nematic matrix. This coupling is the only one allowed by rotational invariance, to lowest order in $d\vec{\mathbf{r}}_j/dz$ and $\delta\vec{\mathbf{n}}$. The potential $V(\vec{\mathbf{r}})$ represents short range, excluded volume effects and can be approximated by $V(\vec{\mathbf{r}})\approx V_0\delta^2(\vec{\mathbf{r}})$. The probability of a particular field configuration is proportional to $\exp(-F/k_BT)$, with $F=F_n+F_p$, and averages are calculated by integrating over both $\delta\vec{\mathbf{n}}(\vec{\mathbf{r}})$ and polymer configurations $\{\vec{\mathbf{r}}_j(z)\}$.

The simplest physical interpretation of the free energy F is of polymers aligned by a nematic solvent with Frank constants $\{K_i\}$. We believe, however, that F also describes *dense* nematic polymers in an *isotropic* solvent. As illustrated in Fig. 1, $\mathbf{n}(\mathbf{r})$ then represents a coarse-grained nematic field obtained by averaging over the polymer tangents in a hydrodynamic averaging volume. Deviations of the orientation of any individual polymer

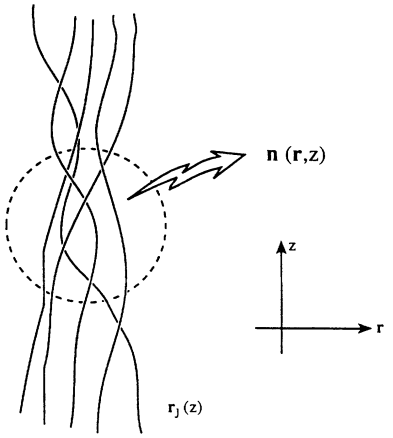

FIG. 1. Hydrodynamic averaging volume surrounding a small region of a nematic polymer containing many polymer strands. The average over the polymer tangents in this volume defines a coarse-grained director field $\mathbf{n}(\vec{r},z)$ which then tends to align the individual polymers that pass through the region.

from this average direction are described by the coupling g. This interpretation of F is especially appropriate for polymers made of nematic molecules connected by flexible hydrocarbon spacers [8,19] as in Fig. 2. In this case $\delta\vec{n}(\mathbf{r})$ describes fluctuations in the orientations of individual nematogens, while $\vec{r}_j(z)$ describes how the nematogens are threaded together by the hydrocarbon spacers. The bare Frank constants in (1.1) are then approximately those of the nematic phase of the unpolymerized nematogens. In this picture, we have [8] $\kappa = K_3/\rho_0$, where ρ_0 is the areal density of polymers cutting a constant-z cross section. Note that the potential $V(\vec{r})$ represents a *scalar* interpolymer interaction within a constant-z plane. The coupling g, when the nematic modes are integrated out, leads to both a scalar interaction, due to the longitudinal modes of the nematic phase, and a *vectorial* interaction, due to the transverse nematic modes (see Sec. VI). In going from the bare polymer system to this coarse-grained system, we could first match the strength of the vectorial interactions with g and then adjust V so as to get the correct strength of the scalar interaction.

Our assumption that polymers interacting with a "nematic-background" field are equivalent to dense nematic polymers in an isotropic solvent is supported by the hydrodynamic approach to correlation functions discussed in Sec. V, which gives identical results for these two systems in the limit of long wavelengths.

FIG. 2. Conventional short-chain nematogens (ellipsoids) connected by hydrocarbon spacers to make a nematic polymer.

The second basic assumption underlying our model calculations is that we can neglect the term proportional to κ in (1.2). To justify this, note first that the initial two terms of (1.2) define a length [8] $\lambda \equiv \sqrt{\kappa/g}$, which for isotropic solvents we identify with the "deflection length" discussed by Odijk [10]. The deflection length is the distance a polymer wanders along z before it feels the confining effect of its neighbors. In order that the polymers order nematically, this length must be less than the polymer persistence length $l_p = \kappa/k_B T$. On scales larger than λ, the coupling to the background nematic field dominates the bending rigidity, and we are justified in neglecting the first term in (1.2). If the deflection length is known, we can express the coupling g in terms of experimental parameters as

$$g = \frac{K_3}{\rho_0 \lambda^2} . \tag{1.3}$$

The equivalence between nematic polymers and polymers in a nematic solvent does *not* extend to the crumpling transition to a more isotropic phase, which should occur in the dilute limit for nematic polymers. The nematic solvent acts like an ordering magnetic field in the latter case, so that the polymer exhibits nematic order at arbitrary dilution. We should also mention that refinements in the model defined by (1.1) and (1.2) are required to handle polymer free ends and hairpins. These are most easily treated after rewriting the theory in a second-quantized "boson" formalism, as discussed in Sec. III.

C. Outline

In Sec. II we first review the wandering of a single polymer in a nematic solvent, assuming initially that hairpin turns can be neglected. In an external field, the polymer just executes a Gaussian random walk in the xy plane as it meanders down the z axis. When the field is turned off, the Goldstone modes of the nematic matrix induce logarithmically divergent "superdiffusive" behavior, as first pointed out by de Gennes [8]. We then generalize the model to include hairpins, using an effective-field-theory method introduced by Cardy [29]. The hairpins cause the polymer to crumple and execute an anisotropic three-dimensional Gaussian random walk. We also discuss polymers wandering in a two-dimensional nematic solvent. Below the Kosterlitz-Thouless transition of the solvent, we find that the polymer exhibits a *continuously variable* Flory exponent, which is simply related to the decay of order in the orientations of the solvent molecules.

In Sec. III we show how to solve the model when many interacting aligned polymers are present via a mapping onto the quantum mechanics of two-dimensional bosons. The constraints imposed on the theory by rotational invariance are discussed in Appendix A. Adding a source

to the boson field theory allows us to obtain analogous results for polymers of finite length. In Sec. IV we calculate the polymer density correlation functions and discuss the renormalized wave-vector-dependent elastic constants.

In Sec. V we generalize the hydrodynamic approach of de Gennes [30] and of Selinger and Bruinsma [31] to allow for polymer heads and tails and show that the results agree with the long-wavelength limit of our more microscopic calculations. In Appendix B we show explicitly how to derive the hydrodynamic theory directly from the boson formalism. We also use the hydrodynamic theory to discuss the physical meaning of the "boson" order parameter used in Sec. III and to calculate the elastic energy of a chain end.

The behavior in the dilute limit is discussed in Sec. VI. We construct renormalization-group recursion relations and show how polymer wandering is affected by both nematic Goldstone modes and interpolymer interactions. In Sec. VII we then introduce hairpins and show that an Ising-like phase transition then describes the dilute limit.

II. A SINGLE CHAIN IN A NEMATIC MATRIX

A. Three dimensions: the de Gennes approximation

With the problem of the nematic polymer in mind, de Gennes introduced the following free energy for a single chain without hairpins in a nematic solvent in the one Frank constant approximation ($K=K_1=K_2=K_3$) [8]:

$$F_1=\tfrac{1}{2}\kappa\int dz\left|\frac{d^2\vec{r}}{dz^2}\right|^2+\tfrac{1}{2}g\int dz\left|\frac{d\vec{r}}{dz}-\delta\vec{n}(\vec{r}(z),z)\right|^2 +\tfrac{1}{2}K\int d^3r|\nabla\delta\vec{n}|^2 . \tag{2.1}$$

The form of the polymer–nematic-matrix coupling comes from the small-tipping-angle expansion of

$$\tfrac{1}{2}g\left[1-\left|\frac{d\mathbf{R}(z)}{dz}\cdot\mathbf{n}(\mathbf{R}(z))\right|^2\right] ,$$

which is the only leading-order coupling consistent with rotational invariance and the discrete $\mathbf{n}\rightarrow-\mathbf{n}$ symmetry. We use $d\mathbf{R}/dz\approx(d\vec{r}/dz,1)/\sqrt{1+|d\vec{r}/dz|^2}$, and $\mathbf{n}=(\delta\vec{n},1)/\sqrt{1+|\delta\vec{n}|^2}$ to find that

$$\left|\frac{d\mathbf{R}}{dz}\cdot\mathbf{n}\right|^2\approx1-\left|\frac{d\vec{r}}{dz}-\delta\vec{n}\right|^2 \tag{2.2}$$

which leads to the coupling displayed in (2.1).

For a fixed configuration of the polymer, the nematic matrix is distorted and some elastic energy results (see Fig. 3). We wish to compute the effective free energy of the chain resulting from integrating out the nematic field in (2.1). Although all terms in (2.1) are quadratic, this problem is, in fact, quite nonlinear due to the appearance of $\vec{r}(z)$ in the argument of $\delta\vec{n}(\vec{r}(z),z)$ of the coupling term. A natural approximation, implicit in de Gennes's discussion [8], is to set $\vec{r}(z)\simeq\vec{0}$ and to discuss only the effect of the fluctuations of the tipping angle $d\vec{r}/dz$. This amounts to replacing the g coupling in (2.1) by

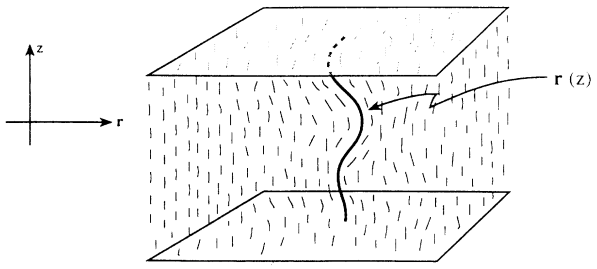

FIG. 3. Isolated polymer in a short-chain nematic solvent. The Goldstone modes of the nematic matrix produce anomalous wandering of the polymer transverse to the z axis.

$$\frac{g}{2}\int dz\left|\frac{d\vec{r}}{dz}-\delta\vec{n}(\vec{r}(z),z)\right|^2\rightarrow\frac{g}{2}\int dz\left|\frac{d\vec{r}}{dz}-\delta\vec{n}(\vec{0},z)\right|^2 , \tag{2.3}$$

where $\delta\vec{n}(\vec{0},z)$ is the value of the distortion of the nematic field on the line $\vec{r}=\vec{0}$. One expects this approximation to be better for large K. A perturbation expansion in K^{-1} of the original problem (2.1) shows that for $d\leq3$, divergent integrals appear, and one must use the renormalization group to obtain correct results. We defer a systematic treatment of this problem to Sec. VI and discuss here only the de Gennes approximation, which can be expected to be qualitatively correct in $d=3$.

The fastest way to compute the effective free energy of the polymer is to note that (2.1) modified by (2.3) can be simplified by the change of variable (with unit Jacobian) $\vec{\eta}(z)=d\vec{r}/dz-\delta\vec{n}(\vec{0},z)$. Upon neglecting the bending energy term, we find that $\vec{r}(z)$ is the solution of

$$\frac{d\vec{r}}{dz}=\delta\vec{n}(\vec{0},z)+\vec{\eta}(z) , \tag{2.4}$$

where $\vec{\eta}(z)$ is a Gaussian white noise of variance k_BT/g. The wandering of the chain is then given by integrating (2.4) over z, squaring and averaging over $\delta\vec{n}(\vec{0},z)$,

$$\langle|\vec{r}(L)-\vec{r}(0)|^2\rangle=\frac{2k_BT}{g}L+\int_0^L\int_0^L dz\,dz'\langle\delta\vec{n}(\vec{0},z)\cdot\delta\vec{n}(\vec{0},z')\rangle_{F_n} . \tag{2.5}$$

Due to the Goldstone mode associated to the rotational invariance of the nematic free energy F_n, the director correlation function decreases like $1/|z-z'|$ at large separations. Upon substituting the full Frank energy (1.1) for the one-Frank-constant term in (2.1) we find (upon setting $H=0$),

$$\langle\delta\vec{n}(\vec{0},z)\cdot\delta\vec{n}(\vec{0},0)\rangle=\frac{k_BT}{4\pi}\left[\frac{1}{K_1}+\frac{1}{K_2}\right]\frac{1}{z} . \tag{2.6}$$

The long-range correlations in the medium then imply via (2.5) "hyperdiffusion" of the chain in the transverse direction

$$\langle |\vec{r}(L)-\vec{r}(0)|^2 \rangle \underset{L\to\infty}{\sim} \frac{2k_BT}{g}L + \frac{k_BT(K_1+K_2)}{2\pi K_1K_2}L\ln(L/a) , \tag{2.7}$$

where a is a microscopic cutoff. The effective diffusion constant [defined by $\langle |\vec{r}(L)-\vec{r}(0)|^2 \rangle = 4D(L)L$] is finite for finite L, but diverges logarithmically as $L\to\infty$,

$$D(L)\equiv \frac{k_BT}{2g}+\frac{k_BT(K_1+K_2)}{8\pi K_1K_2}\ln(L/a) . \tag{2.8}$$

For $K_1=K_2=K$, this is the result obtained by de Gennes by explicitly carrying out the integration over the nematic field [8]. The renormalization-group treatment of Sec. VI (which includes interpolymer interactions) leads to the same result with, however, a factor-of-2 difference in the coefficient of the logarithm.

The nematic solvent is not quite able to produce a finite renormalized diffusion constant for infinitely long polymers. The polymer is still aligned with the z axis on large length scales, however, since $\sqrt{\langle |\vec{r}(L)-\vec{r}(0)|^2 \rangle} \ll L$. It is easy to show that the bending energy, which has been neglected in these calculations, is irrelevant for a single chain without hairpins.

It is interesting to note that, despite its annealed character, this problem is very similar to the problem of random walks in quenched random disorder for which long-range correlations are known to modify diffusion [32].

B. Two dimensions

We now consider the configurations $\vec{r}(s)$ of a chain in a two-dimensional nematic matrix. Although more difficult than its three-dimensional counterpart, an experiment on a two-dimensional surface might be possible: Imagine a long polymer chain with N monomers adsorbed at an air-water interface which is also covered with a tilted monolayer Langmuir-Blodgett film. The projection of the tilted hydrocarbon chains on the plane of the interface plays the role of a director $\vec{n}$, *without* the inversion symmetry $\vec{n}\to-\vec{n}$. We parameterize the direction by $\vec{n}=(\cos\phi, \sin\phi)$. Thermal fluctuations destroy the tilt order above T_c via a Kosterlitz-Thouless [33] vortex unbinding transition. Even below T_c, however, there is no privileged direction in the tilt field since a broken continuous symmetry is impossible in two dimensions for systems with short-range interactions. Thus, one expects the polymer to crumple for $T<T_c$, and one can ask for the wandering exponent ν governing the mean end-to-end distance $R\sim N^{\nu}$, where N is the number of monomers. Note that $\nu=1$ in the three-dimensional problem discussed above. The problem for $d=2$ is nontrivial because below T_c, the nematic field has long-range correlations decaying with a continuously varying exponent:

$$\langle \vec{n}(\vec{x})\cdot\vec{n}(\vec{x}') \rangle = \langle e^{i\phi(\vec{x})}e^{-i\phi(\vec{x}')} \rangle \sim |\vec{x}-\vec{x}'|^{-\eta(T)} . \tag{2.9}$$

The exponent $\eta(T)$ varies from $\eta=0$ at $T=0$ to $\eta=\frac{1}{4}$ at the transition [33]. There are *a priori* two Frank constants K_1 and K_3 in two dimensions, but it has been shown [34] that at large length scales two-dimensional nematic polymers become isotropic ($K_1=K_3=K$) and are described at long wavelengths by the usual XY model free energy $K/2\int dx(\nabla\phi)^2$. For $T<T_c$ one has $\eta=\eta(T)=k_BT/2\pi K$. Above T_c the correlations decay exponentially in (2.9), and then one expects that the wandering exponent of the polymer is the pure self-avoiding-random-walk value $\nu=\frac{3}{4}$ (or $\nu=\frac{1}{2}$ for an ideal chain).

A simple random-walk argument gives an interesting prediction for the exponent ν below T_c. In the infinite-g limit one expects that the polymer by totally aligned with the local field,

$$\frac{dz}{ds}=e^{i\phi(z(s))} , \tag{2.10}$$

where we have used the complex notation for the position $z(s)=x_1(s)+ix_2(s)$, s being the arc length along the polymer. Upon integrating over s we find

$$\langle |z(s)-z(0)|^2 \rangle_{z(0),\phi} = \int_0^s\int_0^s du\,du' \langle e^{i[\phi(z(u))-\phi(z(u'))]} \rangle_{z(0),\phi} , \tag{2.11}$$

where the average is over both initial conditions $z(0)$ for the polymers and over the smoothly varying director angle $\phi(z)$. We now neglect the reaction of the polymer on the nematic field and replace the correlation on the right-hand side of (2.11) by the correlation of the unperturbed nematic field (2.9). This procedure amounts to replacing the problem by that of determining the wandering of the tangent curves of a pure nematic polymer (see Fig. 4). We are led to an integral equation, namely,

$$\langle |z(s)-z(0)|^2 \rangle_{z(0)} = \int_0^s\int_0^s du\,du' \left\langle \frac{\text{const}}{|z(u)-z(u')|^{\eta}} \right\rangle_{z(0)} . \tag{2.12}$$

Upon assuming that $|z(s)-z(0)|$ scales as s^{ν}, we find that the self-consistent value of ν is

$$\nu(T)=\frac{2}{2+\eta(T)} . \tag{2.13}$$

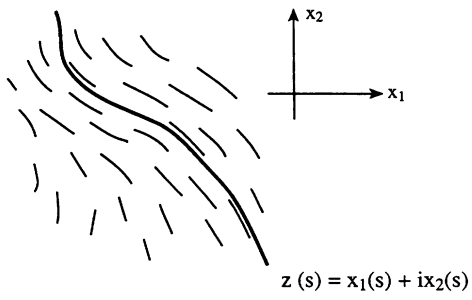

FIG. 4. Polymer interacting with director fluctuations in a two-dimensional nematic medium and described by its complex coordinate z as a function of arclength s.

Our results coincide with those of the Flory theory applied to random walks in quenched random environments, which has been argued to be exact for divergenceless flows [32,35].

According to Eq. (2.13) ν is always close to $\nu=1$, continuously decreasing with increasing temperature from $\nu(T=0)=1$ to $\nu(T=T_c)=\frac{8}{9}$. Note that ν always exceeds $\frac{3}{4}$, the value of a self-avoiding random walk in two dimensions. Our neglect of self-avoidance for $T<T_c$ is thus self-consistent because of the relatively small number of self-intersections that occur for $\nu>\frac{3}{4}$.

C. Field-theoretic treatment of hairpins

In this section we study a *single* polymer embedded in a *rigid* nematic matrix and show that hairpins induce an Ising-like crumpled state. A field theory due to Cardy [29] is used to describe the polymer and introduce hairpins, providing a simplified example of the boson field theory used in later sections. We show explicitly that hairpins cause a single directed polymer to crumple into a more isotropic configuration at long length scales, as suggested in Ref. [8].

Consider the following model free energy for a single polymer in a nematic matrix $\mathbf{n}$:

$$F=\int ds\left[\frac{\kappa}{2}\left[\frac{d\mathbf{T}}{ds}\right]^2-\frac{g}{2}(\mathbf{T}\cdot\mathbf{n})^2\right], \tag{2.14}$$

where $\mathbf{T}=d\mathbf{R}(s)/ds$ is the three-dimensional tangent vector to the polymer and s is the arclength. The first term is the bending energy, while the second represents the lowest order coupling to the background nematic field compatible with overall rotational symmetry. Higher-order terms in $\mathbf{T}$ are possible but are inessential for the following discussion. Note that $|\mathbf{T}|=1$.

Suppose the fluctuations in $\mathbf{n}$ are suppressed by imposing a large magnetic field, so that $\mathbf{n}=\hat{z}$. Then one has

$$F=\int ds\left[\frac{\kappa}{2}\left[\frac{d\mathbf{T}}{ds}\right]^2-\frac{g}{2}(T_z)^2\right], \tag{2.15}$$

which is exactly a continuum one-dimensional Heisenberg model with a quadratic Ising-like anisotropy. As a function of T_z, there are two minima for $T_z=\pm1$. If g is very large, one can expand perturbatively around each minimum. Because this is a one-dimensional problem, the symmetry is in fact restored by tunneling events between the two minima, which correspond to hairpins. T_z thus plays the role of an Ising variable, and hairpins are analogous to an Ising domain wall along the one-dimensional chain. The tunneling probability from one minimum to the next is the energy of a hairpin occurring over a distance R, with energy $\varepsilon_h\approx\min_R(\kappa/2R+gR/2)\sim(g\kappa)^{1/2}$, and the radius of the hairpin is $R_h\sim(\kappa/g)^{1/2}$, which coincides with de Gennes's more elaborate calculation [8]. Note that the size of a hairpin is also of the order of the Odijk deflection length λ [10]. The typical distance between two hairpins along the chain is thus $l\approx ae^{\varepsilon_h/k_BT}$, which can be very large. The statistics of the hairpins is analogous to the statistics of one-dimensional Ising domain walls (with Ising coupling $J\sim\varepsilon_h$). This analogy implies that the length scale a is just the Odijk deflection length. Note that a stretching force applied to the endpoint of the chain is equivalent to an Ising magnetic field, since $\int ds\, hT_z=h[z(L)-z(0)]$. The Ising magnetization is the analog of the total size of the polymer along $\hat{z}$. The elastic modulus G for Hooke's law along $\hat{z}$ is thus given by the Ising susceptibility $G\sim(1/T)e^{J/k_BT}$ as $T\to0$.

The effect of director fluctuations will be discussed in Sec. VII. Here, we continue to neglect them and implement the above ideas with an Ising-like field theory. As noted by Cardy the propagator of a *single* directed polymer of variable length along $\hat{z}$ with two transverse dimensions can be written as the correlation function of a quadratic action, which we write directly in the continuum limit [29],

$$G(\vec{r},\vec{0};z,0)=\frac{1}{Z}\int\mathcal{D}\psi\mathcal{D}\psi^*\psi^*(\vec{0},0)\psi(\vec{r},z)e^{-S_0}, \tag{2.16}$$

where

$$S_0=\int dz\, d^2r\,\psi^*(\partial_z-D\nabla_\perp^2-\bar{\mu})\psi \tag{2.17}$$

with $D=k_BT/2g$. Here

$$G(\vec{r},\vec{0};z,0)=\sum_N W_N(\vec{r},\vec{0};z,0)e^{-\mu N}$$

and $W_N(\vec{r},\vec{0};z,0)$ is the total weight for directed walk of N steps to begin at $(\vec{0},0)$ and end at $(\vec{r},z)$. The chemical potential μ must be adjusted to give the correct polymer size. The use of a retarded propagator only and the neglect of self-interactions if hairpins are excluded has been justified by Cardy. The critical point of this quadratic theory is $\bar{\mu}\to0^-$ corresponding to infinite length chains. The propagator in Fourier space is then

$$G(\vec{q}_\perp,q_z)=\frac{1}{-iq_z+Dq_\perp^2-\bar{\mu}}\equiv G_0(\vec{q}_\perp,q_z). \tag{2.18}$$

Now we discuss a single directed polymer with hairpins but *without* self-avoidance (see Fig. 5). One can in-

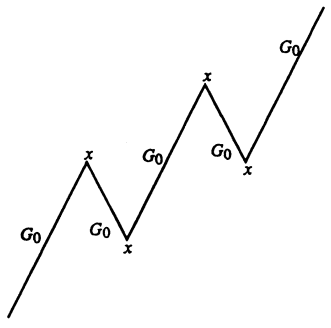

FIG. 5. A directed polymer propagating either up or down the z axis, changing direction whenever a hairpin is present. Each hairpin contributes a factor of $w/2$, and each line contributes a free propagator G_0 to the full propagator G.

troduce hairpins by simply adding to the action (2.17) the term

$$S=S_0-\frac{w}{2}\int dz\, d^2r[\psi^2+(\psi^*)^2]\ , \tag{2.19}$$

which allows for "pair creation." Let us consider the new term as a perturbation and expand in w the above correlation function (2.16). One then generates diagrams as in Fig. 5, with a factor w per hairpin and $G_0(\vec{q}_\perp,q_z)$ per solid line. All closed loops are canceled by the normalization factor Z, so the $n\to 0$ trick is unnecessary. The term of order w^{2n} is the sum of all possible ways to go from $(\vec{0},0)$ to $(\vec{r},z)$ with $2n$ hairpins—the odd terms vanish. The analogy of hairpins with kinks in an Ising-like system shows that we should take $w\propto e^{\varepsilon_h/k_BT}$, with $\varepsilon_h\sim\sqrt{g\kappa}$. If one follows the connected line from $(\vec{0},0)$ the factor associated with the part which represents backward propagation (e.g., after an odd number of hairpins) is actually $G_0^*(\vec{q}_\perp,q_z)$. Thus the sum of all these diagrams is

$$\begin{aligned}G&=G_0(\vec{q}_\perp,q_z)\left[1+\left[\frac{w}{2}\right]^2 G_0G_0^*\right.\\&\quad\left.+\left[\frac{w}{2}\right]^4(G_0G_0^*)^2+\cdots\right]\\&=\frac{G_0}{1-\frac{w^2}{4}G_0G_0^*}\ .\end{aligned} \tag{2.20}$$

Thus the propagator is now

$$G=\frac{iq_z+Dq_\perp^2-\mu}{q_z^2+(Dq_\perp^2-\bar{\mu})^2-\frac{w^2}{4}}\ . \tag{2.21}$$

The critical point has been shifted and is now at $\bar{\mu}=-w/2$. This corresponds physically to the fact that allowing hairpins adds an extra entropy in the system, and the proliferation of paths occurs earlier when $\bar{\mu}$ is raised from $-\infty$. To find the asymptotic large distance behavior, we set $\bar{\mu}=-w/2+\delta\bar{\mu}$ and expand for small $\delta\bar{\mu}$, $\vec{q}_\perp$, and q_z. Then we have

$$G\sim\frac{\frac{1}{2}}{(q_z/w)^2+Dq_\perp^2-\delta\bar{\mu}}\ . \tag{2.22}$$

Note that the complete propagator is actually twice the above result (more precisely it is $G+G^*$) because one has now to allow for graphs where the first propagator in the above series goes backwards. This is the propagator for an (anisotropic) Gaussian random walk in d dimensions. The polymer size now scales as $\sqrt{N}$ both along $\hat{z}$ and along $\vec{r}$, but with an anisotropic radius of gyration tensor. The *directed* nature of the walk has disappeared.

III. FIELD THEORY FOR A LIQUID OF CHAINS WITH A NEMATIC BACKGROUND

In this section we use the analogy with the statistical mechanics of two-dimensional bosons to describe the properties of chains. The details of this analogy are discussed in Refs. [1,36], so we will indicate here only the differences with the case of the flux lines. For a fixed configuration of the nematic solvent, the analogy works as before, except that now the bosons are also interacting with an external "time" and space-dependent field. The average over configurations of the nematic field has to be carried out at the end. We initially discuss the theory for chains that span the system. Internal free ends are then introduced by adding a source to the boson coherent-state field theory. The field theory with the free ends is then used to calculate some important correlation functions in Sec. IV.

A. Mapping onto two-dimensional bosons

We start from the following partition function for the N chains in a nematic field discussed in the Introduction

$$Z_N[\delta\vec{n}]=\frac{1}{N!}\int\prod_{i=1}^{N}\mathcal{D}\vec{r}_i(z)\exp\left[-\frac{1}{k_BT}\int_0^L dz\left[\sum_{i=1}^{N}\frac{g}{2}\left[\frac{d\vec{r}_i}{dz}-\delta\vec{n}(\vec{r}(z),z)\right]^2+\sum_{\substack{i,j=1\\ i<j}}^{N}V(\vec{r}_i(z)-\vec{r}_j(z))\right]\right]\ , \tag{3.1}$$

where we have omitted the bending term and restricted our attention to interactions between lines through an equal "time" potential $V(\vec{r}_i(z)-\vec{r}_j(z))$. The quantity that we are ultimately interested in is the average

$$Z_N=\int\mathcal{D}\,\delta\vec{n}(\vec{r},z)Z_N[\delta\vec{n}]\exp\left[-\frac{F_n}{k_BT}\right]\ , \tag{3.2}$$

where F_n is given by (1.1).

Well-known transformations [37,38] using transfer matrices allow us to write $Z_N[\delta\vec{n}]$ in the Hamiltonian form (first quantization),

$$Z_N[\delta\vec{n}]=\frac{1}{N!}\int d^2r_1\cdots d^2r_N d^2r_1'\cdots d^2r_N'\left\langle\vec{r}_1'\cdots\vec{r}_N'\left|\mathbf{T}\exp\left[-\int dz\frac{\mathcal{H}(z)}{k_BT}\right]\right|\vec{r}_i\cdots\vec{r}_N\right\rangle\ , \tag{3.3}$$

where $|\vec{r}_1 \cdots \vec{r}_N\rangle$ and $|\vec{r}_1' \cdots \vec{r}_N'\rangle$ are states corresponding to the entry and exit points of the polymers [1] and the time ordering operator $\mathbf{T}$ is necessary *a priori* since $\mathcal{H}$ is z dependent. $\mathcal{H}$ can be deduced from the Lagrangian

$$\mathcal{L}(\vec{r}_i,\dot{\vec{r}}_i,z)=\frac{g}{2}\sum_i[\dot{\vec{r}}_i-\delta\vec{n}(\vec{r}_i,z)]^2+\sum_{\substack{i,j\\ i<j}}V(\vec{r}_i-\vec{r}_j) \tag{3.4}$$

according to the usual rules of Euclidean quantum mechanics [37]

$$\mathcal{H}(\vec{p}_k,\vec{r}_k,z)=\mathcal{L}+i\sum_j\vec{p}_j\cdot\dot{\vec{r}}_j\ , \tag{3.5}$$

where $\dot{\vec{r}}_j$ has been eliminated using $\vec{p}_j=i\partial\mathcal{L}/\partial\dot{\vec{r}}_j$. The quantization rule is then $\vec{p}_j=-ik_BT\nabla_j$. We define ∇ so that it operates only within the plane perpendicular to $\hat{z}$. The quantity $\vec{r}$ will always mean a vector perpendicular to $\hat{z}$. Following these rules, we obtain the Hamiltonian for a fixed configuration of $\delta\vec{n}$:

$$\mathcal{H}=\frac{-(k_BT)^2}{2g}\sum_j\nabla_j^2 +k_BT\sum_j\tfrac{1}{2}[\nabla_j\delta\vec{n}(\vec{r}_j,z)+\delta\vec{n}(\vec{r}_j,z)\nabla_j] +\tfrac{1}{2}\sum_{i\neq j}V(\vec{r}_i-\vec{r}_j)\ , \tag{3.6}$$

where we take a symmetrical ordering [37].

A coherent-state representation can now be developed in analogy to the treatment of flux lines in Ref. [1], and one obtains for the grand canonical partition function

$$Z_{\rm gr}\equiv\sum_{N=0}^{\infty}e^{L\mu N/kT}Z_N =\int\mathcal{D}\psi^*(\vec{r},z)\mathcal{D}\psi(\vec{r},z)\mathcal{D}\,\delta\vec{n}(\vec{r},z) \times\exp(-S[\psi^*,\psi,\delta\vec{n}])\ , \tag{3.7}$$

where $\psi(\vec{r},z)$ is a complex boson field. The boson action S reads

$$S=\int_0^L dz\int d^2r\left[\psi^*(\vec{r},z)\left(\frac{\partial}{\partial z}-D\nabla_\perp^2-\bar{\mu}\right)\psi(\vec{r},z)+\tfrac{1}{2}[\psi^*(\vec{r},z)\nabla_\perp\psi(\vec{r},z)-\psi(\vec{r},z)\nabla_\perp\psi^*(\vec{r},z)]\cdot\delta\vec{n}(\vec{r},z) +\tfrac{1}{2}\int d^2r'\bar{v}(\vec{r}-\vec{r}')|\psi(\vec{r},z)|^2|\psi(\vec{r}',z)|^2\right]+\frac{F_n[\delta\vec{n}]}{k_BT}\ . \tag{3.8}$$

Similar manipulations show that the density of flux lines is

$$\rho(\vec{r},z)=|\psi(\vec{r},z)|^2\ , \tag{3.9}$$

where $D=k_BT/2g$, $\bar{\mu}=\mu/k_BT$, and $\bar{v}=V/k_BT$. In Sec. IV we shall calculate correlations in the density $\rho(\vec{r},z)=\sum_{i=1}^N\delta[\vec{r}-\vec{r}_i(z)]$ which may be calculated via the identification (3.9). In the mean-field approximation, we have $\rho_0=\langle|\psi|^2\rangle=\bar{\mu}/\bar{v}$. The field theory embodied in (3.8) differs from the action for flux lines [1] only in the coupling of the boson current $\psi^*\nabla_\perp\psi-\psi\nabla_\perp\psi^*$ to the director field. As discussed in Appendix A, rotational invariance of the original Lagrangian model (3.1) (i.e., Lorentz invariance of the fictitious bosons) forces the coefficient of $(\psi^*\nabla_\perp\psi-\psi\nabla_\perp\psi^*)\cdot\delta\vec{n}$ to be exactly half that of $\psi^*\partial_z\psi$ in the second-quantized coherent-state representation.

B. Effects of finite chain length

To allow for polymers of finite length, which start and stop in the interior of the sample, we add a source term to (3.8)

$$S\to S-h\int dz\int d^2r(\psi+\psi^*)\ . \tag{3.10}$$

Upon replacing ψ and ψ^* by their mean-field average value $\sqrt{\rho_0}$, we see that the quantity $h\sqrt{\rho_0}$ is the probability per unit area and per unit "time" z of starting or terminating a polymer. Since an average of one polymer will thread a cross-sectional area ρ_0^{-1} perpendicular to z, the typical polymer length associated with this Poisson-like process is $l=\sqrt{\rho_0}/h$.

A more formal proof of the equivalence of bosons with a source to the statistical mechanics of directed polymers of finite length can be constructed along the lines taken for isotropic polymer melts [39,40]. We first expand the partition function associated with (3.8) in h, $\bar{v}$, and the nonlinear coupling to the director field. The Fourier-transformed propagator in the resulting Feynman diagrams (see Fig. 5) is

$$G_0(\vec{q}_\perp,q_z)=\frac{1}{-iq_z+Dq_\perp^2}\ , \tag{3.11}$$

or in real space

$$G_0(\vec{r},z)\equiv\langle\psi(\vec{r},z)\psi^*(\vec{0},0)\rangle_0 =\Theta(z)\frac{1}{4\pi Dz}e^{-r^2/4Dz}\ , \tag{3.12}$$

where $\Theta(z)$ is the step function. The expectation value in (3.12) is taken with respect to the Gaussian action

$$S_0=\int_0^L dz\int d^2r[\psi^*(\partial_z-D\nabla_\perp^2)\psi]\ . \tag{3.13}$$

Equation (3.12) is identical to the propagator used in the polymeric description of flux lines presented in Ref. [1]. We can think of $\psi^*(\vec{0},0)$ as creating a polymer at $(\vec{0},0)$

and $\psi(\vec{r},z)$ as destroying a polymer at $(\vec{r},z)$. Although this produces the usual diffusive-random-walk propagator for $z>0$, $G_0(\vec{r},z)=0$ when $z<0$, showing that propagation backwards in the timelike variable z is impossible.

The grand canonical partition function may now be expressed formally as

$$Z_{\rm gr}=\sum_{N_m=0}^{\infty}\sum_{p=0}^{\infty}\mathcal{Z}^{p}_{N_m}(D,\bar{v},K_i)e^{\bar{\mu}L_m}h^{2p}\ , \tag{3.14}$$

where $\mathcal{Z}^{p}_{N_m}(D,\bar{v},K_i)$ is the partition function for N_m monomers distributed among p polymers and $L_m\propto N_m$ is the *total* length along $\hat{z}$ occupied by the N_m monomers. Note that h^2 plays the role of a polymer fugacity, while e^{μ} controls the density of monomers. Figure 6 shows a typical contribution to $\mathcal{Z}^{p}_{N_m}$ of order h^8. The solid lines are the polymer propagator $G_0(\vec{q}_\perp,q_z)$ discussed above. Dashed lines represent the interaction potential $V(\vec{r})$, while the dotted lines signify interactions induced by the background nematic field. The retarded nature of the propagators ensures that large numbers of "unphysical" graphs disappear. The graph shown in Fig. 7(a), for example, with zero momenta on its external legs, is proportional to

$$\frac{1}{(2\pi)^3}\int dq_z d^2q_\perp\frac{|V(\vec{q}_\perp)|^2}{(-iq_z+Dq_\perp^2)^2}\ , \tag{3.15}$$

which vanishes because both poles in the q_z integration are on the same side of the real axis. The graph shown in Fig. 7(b) does not contribute for similar reasons. The graphs shown in Fig. 7(c) are constants that can be absorbed into a redefinition of the chemical potential.

By using the expansion (3.14), we can easily show that the average polymer length is given by

$$\langle L_m\rangle=\frac{\partial}{\partial\bar{\mu}}\ln Z_{\rm gr}=\frac{\sum_{N_m=0}^{\infty}\sum_{p=0}^{\infty}L_m\mathcal{Z}^{p}_{N_m}(D,\bar{v},K_i)e^{\bar{\mu}L_m}h^{2p}}{Z_{\rm gr}}\ , \tag{3.16}$$

while the average number of polymers is

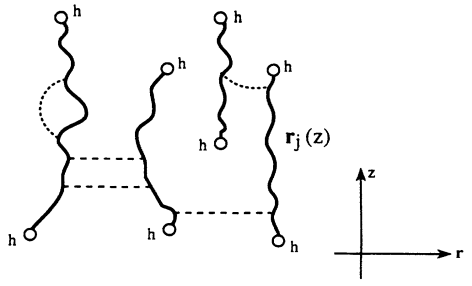

FIG. 6. Contribution to order h^8 to the polymer-generating function. Solid lines are the polymer propagators $G_0(\vec{q}_\perp,q_z)$. Dashed lines represent the interaction potential $V(\vec{r})$, while the dotted lines represent interactions induced by the background nematic field.

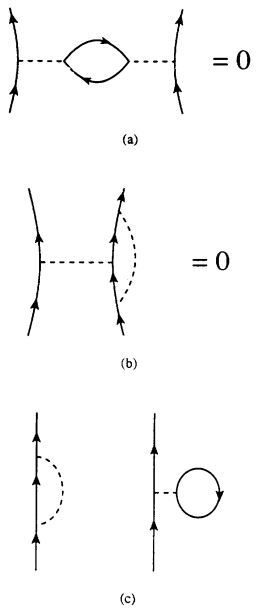

FIG. 7. Ingredients of the graphical perturbation theory described in the text. (a) and (b) Contributions to the renormalized interpolymer interaction potential which vanish due to the retarded nature of the polymer propagator. (c) The terms shown are constants that can be absorbed into a shift in the chemical potential.

$$\langle p\rangle=h^2\frac{\partial}{\partial(h^2)}\ln Z_{\rm gr}=\frac{\sum_{N_m=0}^{\infty}\sum_{p=0}^{\infty}p\mathcal{Z}^{p}_{N_m}(D,\bar{v},K_i)e^{\bar{\mu}L_m}h^{2p}}{Z_{\rm gr}}\ . \tag{3.17}$$

We can now calculate the typical polymer length

$$l\equiv\langle L_m\rangle/\langle p\rangle=\frac{\langle|\psi(\vec{r},z)|^2\rangle}{(h/2)\langle\psi(\vec{r},z)+\psi^*(\vec{r},z)\rangle} \tag{3.18}$$

directly from the mean-field approximation to the partition function (3.7). We assume for simplicity the contact potential $V(\vec{r})=k_BT\bar{v}\delta^2(\vec{r})$. Upon making the substitution (3.10) in (3.7) and setting $\psi(\vec{r},z)$ to a constant value $\psi=\psi^*=\psi_0=\sqrt{\rho_0}$, we have

$$\ln Z_{\rm gr}=-\Omega\min_{\psi_0}(-\mu\psi_0^2+\tfrac{1}{2}\bar{v}\psi_0^4-2h\psi_0)\ , \tag{3.19}$$

where Ω is the (three-dimensional) volume. There are two limiting cases to consider. When $\bar{\mu}\gg0$, we assume an ordered state only slightly perturbed by the small source field h. As we shall see, this means restricting our attention to very long chains. The minimum of (3.19) is then given to lowest order in h by

$$\psi_0\approx\sqrt{\bar{\mu}/\bar{v}}\,(1+\sqrt{\bar{v}/\bar{\mu}^3}h/2)\ , \tag{3.20}$$

while the partition function is

$$Z_{\rm gr}=\exp\left[\Omega\left[\frac{\bar{\mu}^2}{2\bar{v}}+2h\sqrt{\bar{\mu}/\bar{v}}\right]\right]\ . \tag{3.21}$$

We then find from (3.16) and (3.17) that

$$\langle L_m \rangle \approx \psi_0^2 \Omega \tag{3.22}$$

and

$$\langle p \rangle \approx \psi_0 h \Omega \ , \tag{3.23}$$

so that a typical length is

$$l \approx \psi_0 / h \ , \tag{3.24}$$

as also follows directly from the mean-field approximation. Note that this length diverges as $h \to 0$ and agrees with the estimate made at the beginning of this section.

If $\bar{\mu} \lesssim 0$, the polymers are dilute, and we are in the disordered phase of the model. We assume that polymers follow an imposed external direction, as in electrorheological fluids, so that we need not worry about the crumpling transition discussed in the Introduction. One can then neglect $\bar{v}$ and find that the order parameter is

$$\psi_0 \approx h / |\bar{\mu}| \ , \tag{3.25}$$

while the grand partition function is

$$\mathcal{Z}_{\rm gr} \approx \exp\left[\Omega \left[\frac{h^2}{|\bar{\mu}|}\right]\right] . \tag{3.26}$$

The total length of polymer is now

$$\langle L_m \rangle = \frac{h^2}{\bar{\mu}^2} \Omega \ , \tag{3.27}$$

while the average number is

$$\langle p \rangle = \frac{h^2}{|\bar{\mu}|} \Omega \ . \tag{3.28}$$

A typical polymer size is thus

$$l \approx \frac{1}{|\bar{\mu}|} \quad (h = 0^+) \ , \tag{3.29}$$

which increases as the transition is approached from negative μ.

Experiments are usually done varying the polymer concentration with a fixed distribution of polymers sizes, and hence, fixed l. This produces the trajectory shown in Fig. 8 on the phase diagram plotted as a function of $-\mu$ and ψ_0. Typical polymer configurations at two points on this phase diagram are indicated. Note that the model corresponds to a *distribution* of chain lengths instead of a monodisperse sample. This is also a feature of the des Cloiseaux model of isotropic polymer melts, for which it is possible to draw a very similar phase diagram [39,40]. A broad distribution of chain lengths is probably a good approximation for electrorheological fluids and ferrofluids, in which the chains are constantly breaking and reforming. The difference between polydisperse and monodisperse samples is not, in any event, expected to be important when the average chain length is large [40].

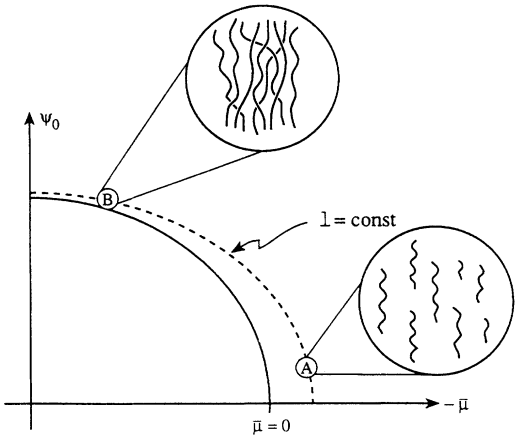

FIG. 8. Phase diagram as a function of the boson order parameter and the chemical potential $\bar{\mu}$. The dashed line represents a contour of constant polymer length. Typical configurations are shown at the points A (dilute) and B (dense and entangled). The solid curve represents the boson order parameter for $h = 0$, and terminates at a critical point that describes the theory in the dilute limit.

IV. RESULTS FOR CORRELATION FUNCTIONS

We now assume that the polymers are dense and entangled, i.e., $\sqrt{Dl} \gg \rho_0^{-1/2}$. Correlations for small h can then be calculated as in Refs. [1,36], by expanding about the mean-field order parameter $\psi_0 = \sqrt{\rho_0} \approx \sqrt{\bar{\mu}/\bar{v}}\,[1 + O(h)]$.

A. Gaussian form for the action

Let us write the complex field $\psi(\vec{r},z)$ in terms of the density $\rho(\vec{r},z)$ and the phase $\theta(\vec{r},z)$ as

$$\psi(\vec{r},z) = \rho(\vec{r},z)^{1/2} \exp[i\theta(\vec{r},z)] \ . \tag{4.1}$$

The measure takes the simple form, up to unimportant constant factors

$$\mathcal{D}\psi^*(\vec{r},z)\mathcal{D}\psi(\vec{r},z) = \mathcal{D}\rho(\vec{r},z)\mathcal{D}\theta(\vec{r},z) \ . \tag{4.2}$$

To simplify the discussion, let us again consider a contact potential $V(\vec{r}) = V_0 \delta^2(\vec{r})$ and set $\bar{v} = V_0 / k_B T$. The action then takes the form in the new variables

$$S = \int dz\, d^2 r \left[i\rho \partial_z \theta + \frac{D}{4\rho} (\nabla_\perp \rho)^2 + D\rho (\nabla_\perp \theta)^2 + i\rho \nabla_\perp \theta \cdot \delta\vec{n} - \bar{\mu}\rho + \tfrac{1}{2}\bar{v}\rho^2 - 2h\rho^{1/2}\cos\theta \right] + \frac{F_n[\delta\vec{n}]}{k_B T} \ . \tag{4.3}$$

Upon setting $\rho(\vec{r},z) = \rho_0 + \delta\rho(\vec{r},z)$, where $\rho_0 = \psi_0^2$ is given by (3.20), and expanding to quadratic order the fluctuations $\delta\rho$ and θ, the action becomes, up to total derivatives and constants,

$$S=\int dz\, d^2r \left[i\delta\rho\partial_z\theta+\frac{D}{4\rho_0}(\nabla_\perp\delta\rho)^2+D\rho_0(\nabla_\perp\theta)^2 +i\rho_0\nabla_\perp\theta\cdot\delta\vec{n}+\tfrac{1}{2}\bar{v}(\delta\rho)^2+h\rho_0^{1/2}\theta^2 +\tfrac{1}{2}h\rho_0^{-3/2}(\delta\rho)^2 \right] . \tag{4.4}$$

Note that the term involving $\delta\vec{n}$ can be rewritten as $-i\rho_0\theta(\nabla_\perp\cdot\delta\vec{n})$, so that only the longitudinal part of $\delta\vec{n}$ couples to the polymer degrees of freedom.

Upon expanding the fields in Fourier modes

$$\theta(\vec{r},z)=(\Omega)^{-1/2}\sum_{\vec{q}_\perp,q_z} e^{izq_z+i\vec{q}_\perp\cdot\vec{r}}\theta(\vec{q}_\perp,q_z) , \tag{4.5}$$

with similar expansions for $\delta\rho$ and $\delta\vec{n}$, one obtains the action

$$S=\tfrac{1}{2}\sum_{\vec{q}_\perp,q_z} X^+(\vec{q}_\perp,q_z)G^{-1}(\vec{q}_\perp,q_z)X(\vec{q}_\perp,q_z) , \tag{4.6}$$

where $X\equiv(\theta,\delta\rho,\delta n_x,\delta n_y)$ and [taking $H=0$ in (1.1) for simplicity],

$$G^{-1}=\begin{bmatrix} \left(2D\rho_0q_\perp^2+2h\rho_0^{1/2}\right) & -q_z & -\rho_0q_x & -\rho_0q_y \\ q_z & \left[\frac{D}{2\rho_0}q_\perp^2+\bar{v}+h\rho_0^{-3/2}\right] & 0 & 0 \\ \rho_0q_x & 0 & \frac{(K_1q_x^2+K_2q_y^2+K_3q_z^2)}{k_BT} & \frac{K_1-K_2}{k_BT}q_xq_y \\ \rho_0q_y & 0 & \frac{K_1-K_2}{k_BT}q_xq_y & \frac{(K_1q_y^2+K_2q_x^2+K_3q_x^2)}{k_BT} \end{bmatrix} . \tag{4.7}$$

It is now straightforward to calculate any desired correlation function, by inverting this 4×4 matrix.

B. Discussion of correlations

The structure function

$$S(\vec{q}_\perp,q_z)=\langle|\delta\rho(\vec{q}_\perp,q_z)|^2\rangle \tag{4.8}$$

may be written

$$S(\vec{q}_\perp,q_z)=\rho_0\frac{\rho_0q_\perp^2+2\bar{K}(\mathbf{q})(l^{-1}+Dq_\perp^2)}{\bar{K}(\mathbf{q})[q_z^2+\bar{\epsilon}^2(q_\perp)]+\frac{1}{2}\rho_0q_\perp^2\bar{\epsilon}^2(q_\perp)/(l^{-1}+Dq_\perp^2)} , \tag{4.9}$$

where

$$\bar{K}(\mathbf{q})=\frac{K_1q_\perp^2-K_3q_z^2}{k_BT} . \tag{4.10}$$

We have set $\rho_0^{1/2}/h=l$, and

$$\bar{\epsilon}^2(q_\perp)=(l^{-1}+Dq_\perp^2)(l^{-1}+Dq_\perp^2+2\rho_0v) . \tag{4.11}$$

To obtain results for arbitrary in-plane pair potentials $V(\vec{r})$, let $\bar{v}\to\hat{V}(\vec{q}_\perp)/k_BT$, where $\hat{V}(\vec{q}_\perp)$ is the Fourier transform of $V(\vec{r})$. Unlike its flux-line counterpart, the Bogoliubov spectrum (4.11) has a gap as $q_\perp\to0$, due to the finite polymer lengths. Upon evaluating $\langle\delta n_i(\mathbf{q})\delta n_j(-\mathbf{q})\rangle$, we determine the renormalized Frank constant via the identification

$$\langle\delta n_i(\mathbf{q})\delta n_j(-\mathbf{q})\rangle=\frac{1}{K_2^Rq_\perp^2+K_3^Rq_z^2}P_{ij}^T+\frac{1}{K_1^Rq_\perp^2+K_3^Rq_z^2}P_{ij}^L . \tag{4.12}$$

K_2 and K_3 are unrenormalized, while

$$K_1^R(\vec{q}_\perp,q_z)=K_1+\tfrac{1}{2}\rho_0k_BT\frac{\bar{\epsilon}(q_\perp)}{q_z^2+\bar{\epsilon}^2(q_\perp)}\frac{1}{(l^{-1}+Dq_\perp^2)} . \tag{4.13}$$

Upon taking the limit $\bar{K}(\mathbf{q})\to\infty$, which suppresses all fluctuations in the director field, (4.9) can be applied to polymer melts with an externally imposed average direction. In the limit of small wave vectors, the structure function takes the simple form,

$$S(\vec{q}_\perp,q_z)=k_BT\frac{\rho_0^2q_\perp^2+K/G}{Bq_\perp^2+Kq_z^2+G^{-1}KB\rho_0^{-2}} , \tag{4.14}$$

where $B=\rho_0^2V_0+O(l^{-1})$ is a two-dimensional bulk modulus, $K=\rho_0g$ is a tilt modulus, and G is related to the average length via $G=lk_BT/2\rho_0$. When $l\to\infty$ the structure function contours are straight lines passing through the origin, with no scattering along the line

$q_\perp=0$ [6,7]. Scattering reappears at $q_\perp=0$ for finite l, however. Fits of (4.14) to scattering data should allow a simple direct determination of the average chain length l and the important parameters B and K.

The small-wave-vector limit of (4.9) when the Frank constants are finite has a different form

$$S(\vec{q}_\perp,q_z)=k_BT\frac{\rho_0^2q_\perp^2+(K_1q_\perp^2+K_3q_z^2)/G}{Bq_\perp^2+(B/G\rho_0^2+q_z^2)(K_1q_\perp^2+K_3q_z^2)} . \tag{4.15}$$

When $G=lk_BT/2\rho_0\to\infty$, (4.15) reduces to the prediction [31] of a hydrodynamic theory due to de Gennes [30]. Finite-length effects distort the contours near the origin, however, and are likely to be quite important in fitting real scattering data. Fits to (4.15) should lead to direct experimental determination of the Frank constant, the bulk modulus B, and the mean polymer length. Upon taking the limit $\mathbf{q}\to 0$ in (4.13) we find the dependence on the renormalized splay elastic constant K_1^R on the polymer length,

$$K_1^R=K_1+\tfrac{1}{2}k_BTl\rho_0 , \tag{4.16}$$

in agreement with a prediction of Meyer [9], but in disagreement with a suggestion by de Gennes [8].

V. HYDRODYNAMIC TREATMENT OF CORRELATIONS

The hydrodynamic description of isotropic liquids of atoms or small molecules has been understood for many years [41]. The long-wavelength density fluctuations are Gaussian, and static correlation functions are described by Ornstein-Zernike theory [42]. We generalize here an analogous theory of liquids of oriented lines in three dimensions. The basic concepts were first discussed by de Gennes and Meyer in the context of polymer nematic liquid crystals over a decade ago [8,9]. These ideas were recently used to determine the form of the liquid-crystal structure function near the origin of reciprocal space by Selinger and Bruinsma [31]. The hydrodynamic theory can in fact be derived directly from the boson representation, as shown in Appendix B. We show here how a finite density of chain lengths can be incorporated in a natural way for ferro- and electrorheological fluids, as well as for nematic polymers. The results agree in all cases with the long-wavelength limit of those in Sec. IV. We also use the hydrodynamic theory to show that there are essentially no differences at long wavelengths between polymers in a nematic solvent and dense nematic polymers in an isotropic solvent. Some of our conclusions were reviewed recently in Ref. [43].

Hydrodynamics will, in addition, allow us to discuss the physical meaning of the boson order parameter introduced in Sec. III. To this end, we calculate the energy of an isolated free end in a ferro- or electrorheological fluid. Such a calculation has already been carried out for nematic polymers by Selinger and Bruinsma [44].

A. Ferro- and electrorheological fluids

We first assume for simplicity that the chains of magnetic or electric dipole particles span the system along the $\hat{z}$ axis. The effects of finite chain length will be discussed later. The basis hydrodynamic fields are now an areal particle density

$$\rho_{\rm mic}(\vec{r},z)=\sum_{j=1}^{N}\delta^2[\vec{r}-\vec{r}_j(z)] \tag{5.1}$$

and a tangent field in the plane perpendicular to $\hat{z}$,

$$\vec{t}_{\rm mic}(\vec{r},z)=\sum_{j=1}^{N}\frac{d\vec{r}_j(z)}{dz}\delta^2[\vec{r}-\vec{r}_j(z)] . \tag{5.2}$$

We coarse grain these microscopic fields to obtain smoothed density and tangent field $\rho(\vec{r},z)$ and $\vec{t}(\vec{r},z)$.

We now expand the free energy of the liquid to quadratic order in the density deviation $\delta\rho(\vec{r},z)=\rho(\vec{r},z)-\rho_0$ and in $\vec{t}(\vec{r},z)$

$$F=\frac{1}{2\rho_0^2}\int d^2r\,dz[B(\delta\rho)^2+K|\vec{t}|^2] . \tag{5.3}$$

The parameter B is a bulk modulus for areal compressions and dilations perpendicular to the z axis, while K is the modulus for tilting lines away from the direction of the applied field. Because we are dealing with *lines*, and not simply oriented anisotropic particles, (5.3) must be supplemented with an equation of continuity,

$$\partial_z\delta\rho+\nabla_\perp\cdot\vec{t}=0 , \tag{5.4}$$

which reflects the fact that vortex lines cannot stop or start inside the medium. Correlation functions can be calculated by assuming that the probability of a particular line configuration is proportional to $\exp(-F/k_BT)$, and imposing the constraint (5.4) on the statistical mechanics.

We now modify (5.3) to allow for chains that stop and start inside the medium. If the chains are long and entangled, we can treat the chain heads and tails as independent ideal gases, following similar ideas for nematic polymers by Meyer [9]. The free energy (5.3) is now replaced by an expansion of the form

$$F=\tfrac{1}{2}\int d^2r\,dz\left[B\left[\frac{\delta\rho}{\rho_0}\right]^2+K\left[\frac{\vec{t}}{\rho_0}\right]^2+G(\partial_z\delta\rho+\nabla_\perp\cdot\vec{t})^2\right] , \tag{5.5}$$

which differs from (5.3) only in a term proportional to the square of the constraint displayed in (5.4). Although other terms proportional to gradients of $\delta\rho$ and $\vec{t}$ can appear, we have kept only those couplings that dominate in the limit of long chains. We can now treat $\delta\rho$ and $\vec{t}$ as independent fields and then take the limit $G\to\infty$ to impose the constraint. The coupling G is finite, however, when the chains are of finite length. To determine the value of G in this case, note that the chain heads and tails act as sources and sinks on the right-hand side of the conservation law (5.4). It follows that [9]

$$\partial_z \delta\rho + \nabla_\perp \cdot \vec{t} = \rho_H - \rho_T \ , \tag{5.6}$$

when finite densities of chain heads $\rho_H(\vec{r},z)$ and chain tails $\rho_T(\vec{r},z)$ are present. If the heads and tails are treated as two noninteracting ideal gases, a term of the form

$$\delta F = \tfrac{1}{2} G \int d^2r\, dz (\rho_H - \rho_T)^2 \tag{5.7}$$

should appear in the free energy. The coefficient is just the concentration susceptibility for an ideal binary mixture, which is well known to be [45]

$$G = \frac{k_B T}{\langle \rho_H \rangle + \langle \rho_T \rangle} \ , \tag{5.8}$$

where $\langle \rho_H \rangle$ and $\langle \rho_T \rangle$ are the average concentrations of heads and tails, respectively. Now, each chain contributes both a head and a tail, $\langle \rho_H \rangle = \langle \rho_T \rangle = \rho_{\text{chain}}$, and the three-dimensional density of chains is $\rho_{\text{chain}} = \rho_0 / l$, where l is a typical chain length. It follows that

$$G = \frac{l k_B T}{2\rho_0} \ , \tag{5.9}$$

which diverges as $l \to \infty$. It is easy to check that the structure function, which results from this hydrodynamic treatment, agrees with the result (4.14) of the more microscopic boson calculations of Sec. III in the long-wavelength limit.

Figure 9 shows the scattering contours expected for dense aligned ferro- or electrorheological fluids. The maxima along the $q_\perp$ axis occur approximately at the position of the first reciprocal-lattice vector in the nearby crystalline phase and are *not* accounted for by the hydrodynamic theory. As discussed in Ref. [1], the half width at half maximum along q_z for fixed $q_\perp$ controls the decay of density fluctuations along the z axis. Hydrodynamics (in agreement with the boson theory) determines the linear form via (4.14) of the contours near the origin. The rounding of these contours (indicated by the dashed lines) due to the finite polymer length is one of the principal predictions of Ref [26] and this paper. When $l \to \infty$, the contours remain linear as $q_\perp, q_z \to 0$, and the scattering vanishes along the q_z axis, as in the case of flux lines [1].

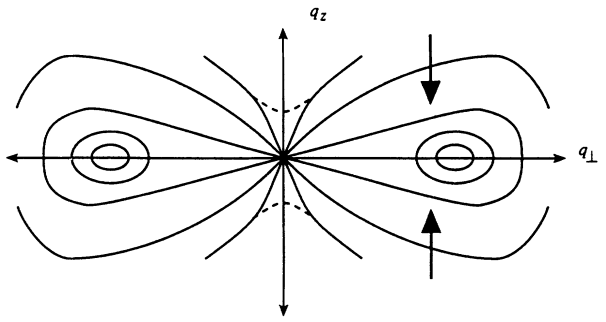

FIG. 9. Contours of constant scattering intensity for long-chain ferro- and electrorheological fluids. The contours are linear near the origin and surround a maximum on the $q_\perp$ axis located approximately at the position of the first Bragg peak of the nearby hexagonal crystalline phase. The linear contours near the origin are rounded by finite chain-length effects.

B. Nematic polymers

The hydrodynamic treatment of infinitely long nematic polymers is due originally to de Gennes [30] and was applied to correlation functions by Selinger and Bruinsma [31]. We first assume an isotropic solvent. The hydrodynamic variables are now the areal polymer density (5.1) and a fluctuating nematic deviation field $\delta\vec{n}(\vec{r},z)$ attached to the polymers. We again allow for a dilute concentration of chain ends by writing the hydrodynamic free energy as

$$F = \tfrac{1}{2} \int d^2r\, dz \left[B \left[\frac{\delta\rho}{\rho_0} \right]^2 + G(\partial_z \delta\rho + \rho_0 \nabla_\perp \cdot \delta\vec{n})^2 \right] + F_n[\delta\vec{n}] \ , \tag{5.10}$$

where F_n is given by (1.1), with $H = 0$ and G must again be given (5.9) in the dilute limit. When $G \to \infty$, we recover the constraint,

$$\partial_z \delta\rho + \rho_0 \nabla_\perp \cdot \delta\vec{n} = 0 \ . \tag{5.11}$$

For finite G, one again finds agreement with correlations calculated from (5.10) and the hydrodynamic limit (4.15) of the result (4.9) obtained from the microscopic boson theory.

Figure 10 shows the hydrodynamic predictions for scattering off the polymers in the limit of small momentum transfer. The structure for larger $q_\perp \sim \rho_0^{-1/2}$ should be similar to that shown near the peaks in Fig. 9 [25]. For infinitely long polymers, the scattering vanishes along the q_z axis, and the contours take the form $q_z \propto q_\perp^{1/2}$ [31]. The boson and hydrodynamic theory prediction (4.15) lead to the rounding indicated by the dashed lines in Fig. 10, an effect which is likely to be quite important in fitting real experimental data.

As discussed in Ref. [43], hydrodynamics also makes interesting predictions about freeze-fracture experiments on directed polymer melts. It can be shown, in particular, that density fluctuations measured in a fracture plane perpendicular to $\hat{z}$ provide a precise signature that one is dealing with a liquid of lines rather than a liquid of

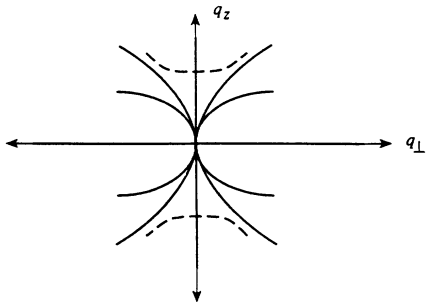

FIG. 10. Contours of constant scattering intensity near the origin for nematic polymers. The characteristic square-root contours are rounded off as indicated by the dashed lines unless the polymers are very long.

points. Under favorable circumstances, it is even possible to determine a typical polymer length from such measurements.

We can also treat polymers in a *nematic* solvent using hydrodynamics, and check that there are no significant differences with conventional nematic polymers in the long-wavelength limit. The (unpolymerized) nematic solvent will now be described by the free energy (1.1), and we introduce coarse-grained polymer variables as in (5.1) and (5.2). The hydrodynamic free energy (as derived explicitly in Appendix B) is then

$$F'=\frac{1}{2}\int d^2r\,dz\left[B\left[\frac{\delta\rho}{\rho_0}\right]^2+g|\vec{t}-\rho_0\delta\vec{n}|^2+G(\partial_z\delta\rho+\nabla_\perp\cdot\vec{t})^2\right]+F_n[\delta\vec{n}]\ , \tag{5.12}$$

where the coupling proportional to g reflects the analogous coupling in (2.1). We now integrate out the solvent degrees of freedom, which leads to an effective free energy

$$e^{-F'_{\rm eff}/k_BT}=\int \mathcal{D}\,\delta\vec{n}\,e^{-F'/k_BT} \tag{5.13}$$

given by

$$F'_{\rm eff}=\frac{1}{2}\int d^2r\,dz\left[\left[\frac{\delta\rho}{\rho_0}\right]^2+G(\partial_z\delta\rho+\nabla_\perp\cdot\vec{t})^2\right]+F'_n[\vec{t}] \tag{5.14}$$

where

$$F'_n[\vec{t}]=\frac{1}{(2\pi)^d}\frac{1}{2\pi}\int d^dq_\perp dq_z\left[g\frac{K_1q_\perp^2+K_3q_z^2}{K_1q_\perp^2+K_3q_z^2+g\rho_0^2}\frac{q_\perp^iq_\perp^j}{q_\perp^2}+g\frac{K_2q_\perp^2+K_3q_z^2}{K_2q_\perp^2+K_3q_z^2+g\rho_0^2}\frac{\delta^{ij}-q_\perp^iq_\perp^j}{q_\perp^2}\right]t_i(\mathbf{q})t_j(-\mathbf{q})\ . \tag{5.15}$$

At long wavelengths, the coefficients of the longitudinal and transverse projectors in (5.15) simplify, and F'_n for polymers in a nematic solvent reduces to the F_n appropriate for conventional nematic polymers. The two systems are indeed equivalent from the point of view of long-wavelength polymer correlation functions.

C. Defect energies and the boson order parameter

Hydrodynamics also allows us to better understand the boson order parameter used in Secs. III and IV. For an analogous discussion for flux lines in high-T_c superconductors, see Ref. [2]. Note that the representation (4.1) only makes sense if there is phase coherence in the equivalent "boson" system. Consider the correlation function

$$G(\vec{r},\vec{r}';z,z')=\langle\psi(\vec{r},z)\psi^*(\vec{r}',z')\rangle\ , \tag{5.16}$$

where $\psi(\vec{r},z)$ and $\psi^*(\vec{r}',z')$ are, respectively, creation operators for polymer heads and tails. We assume that the polymers are long and entangled, so that $h=0$ in (3.10). Phase coherence means long-range order in $G(\vec{r},\vec{r}';z,z')$, for fixed z and z',

$$\lim_{|\vec{r}-\vec{r}'|\to\infty} G(\vec{r},\vec{r}';z,z')=\text{const}>0\ . \tag{5.17}$$

To understand what this long-range order means, consider first the behavior of (5.16) in a hexagonal *crystal* of directed polymers, with the strands again aligned with the z axis. The composite operator in (5.16) creates an extra line at $(\vec{r}',z')$ (i.e., a column of interstitials in the solid), and destroys an existing line at $(\vec{r},z)$, creating a column of vacancies. As shown in Fig. 11, the lowest energy configuration is then a line of vacancies (for $z'>z$) or interstitials (for $z'<z$) connecting the two points with an energy σs proportional to the length s of this "string." The string tension σ will depend on the angle θ this line

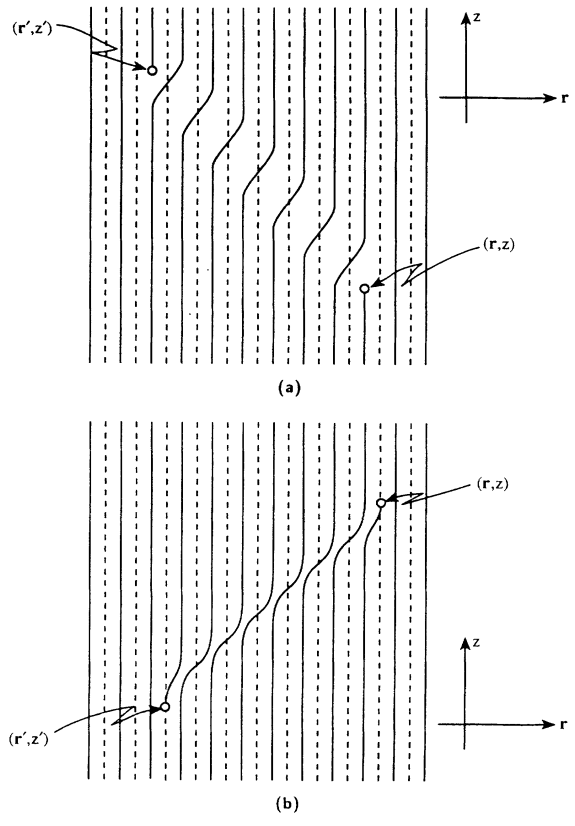

FIG. 11. Lowest-energy solid phase contribution to the correlation function $G(\vec{r},\vec{r}';z,z')$, which inserts a flux head and tail into a crystalline polymer array. Dashed lines represent a row of polymers slightly behind the plane of the page. (a) A vacancy is created at time z, which then propagates and is destroyed at time z'. Interstitial propagation from z' to z is shown (b). The energy of the "string" defect connecting the head to the tail increases linearly with the separation in both cases and leads to the exponential decay of $G(\vec{r},\vec{r}';z,z')$.

makes with the z axis. It follows that the correlation function (5.16) decays exponentially to zero (i.e., like $\exp[-\sigma(\theta)s/k_BT]$) for large separations in this crystalline phase. In a directed polymer *melt,* on the other hand, the concept of vacancy and interstitial lines has no meaning, and the string tension σ will vanish for large s, implying long-range order in $G(\vec{r},\vec{r}';z,z')$ as $|\vec{r}-\vec{r}'|\to\infty$.

Long-range order in the boson order parameter $\psi(\vec{r},z)$ means that

$$\langle\psi(\vec{r},z)\rangle=\langle\psi^*(\vec{r},z)\rangle\propto e^{-E^*/k_BT}>0\ . \tag{5.18}$$

Here, E^* is the energy of an isolated polymer head or tail. The hydrodynamic theory provides a transparent demonstration that unlike hexagonal crystals, this energy is finite. This energy has already been calculated by Selinger and Bruinsma for nematic polymers [44], so we concentrate here on the hydrodynamics for ferro- and electrorheological fluids. The constraint (5.4) applies everywhere away from an isolated head or tail and is conveniently implemented by expressing $\delta\rho$ and $\vec{t}$ in terms of a two-component displacement field $\vec{u}(\vec{r},z)$,

$$\delta\rho=-\rho_0\vec{\nabla}_\perp\cdot\vec{u}\ , \tag{5.19a}$$

$$\vec{t}=\rho_0\frac{\partial\vec{u}}{\partial z} \tag{5.19b}$$

following a similar method by Taratura and Meyer [46] for nematic polymers. The free energy becomes

$$F=\tfrac{1}{2}\int dz\,d^2r[B(\nabla_\perp\cdot\vec{u})^2+K(\partial_z\vec{u})^2]\ . \tag{5.20}$$

The extremal equations associated with (5.20) for an isolated polymer head at the origin are

$$B\nabla_\perp(\nabla_\perp\cdot\vec{u})+K\partial_z^2\vec{u}=B\rho_0^{-1}\Theta(z)\nabla_\perp\delta^2(\vec{r})\ , \tag{5.21}$$

where ρ_0 is the average in-plane polymer density and $\Theta(z)$ is the step function $\Theta(z)=1$, $z>0$ and $\Theta(z)=0$, $z<0$. See Ref. [47] for a discussion of the source term for the closely related problem of a dislocation in a two-dimensional smectic liquid crystal. Here, the source represents the absence of a line along the positive z axis. In a crystal, this line would be a string of vacancies, and its energy would be infinite, due to the disruption of the crystalline order parameter in the vicinity of the line. In a liquid, however, the vacancy free energy vanishes, and we need only consider the long-range strain field associated with (5.21). Upon solving (5.21) in Fourier space, we find

$$\vec{u}(\vec{q}_\perp,q_z)=\frac{-(B/\rho_0)\vec{q}_\perp}{q_z(Bq_\perp^2+Kq_z^2)}\ , \tag{5.22}$$

which leads to an explicit expression for the tilt field

$$\vec{t}=\rho_0\partial_z\vec{u}=\frac{B^{1/2}K}{4\pi}\frac{\vec{r}}{(Kr^2+Bz^2)^{3/2}}\ . \tag{5.23}$$

The density perturbation associated with the free end is

$$\delta\rho=-\rho_0(\nabla_\perp\cdot\vec{u})=\frac{-B^{3/2}K}{4\pi}\frac{z}{(Kr^2+Bz^2)^{3/2}}\ . \tag{5.24}$$

Since both these strains fall off like $1/(\text{distance})^2$ far from the origin, the integrated strain energy in (5.18) is indeed finite, i.e.,

$$E^*<\infty\ , \tag{5.25}$$

where we have included a microscopic short-range contribution in the defect energy E^*.

The analysis for nematic polymers [44] is more complicated but also leads to the conclusion that the energy of an isolated head or tail is finite, consistent with a nonzero value of the boson order parameter. The strains in (5.23) and (5.24) resemble those expected for a magnetic monopole in an anisotropic medium. Indeed, (5.4) is just the condition of "no magnetic monopoles," $\nabla\cdot\mathbf{b}=0$, if we identify $\delta\rho$ with b_z and $\vec{t}$ with $\vec{b}_\perp$, while (5.3) is just the magnetic field energy of a medium with an anisotropic permeability. The energy of isolated magnetic monopoles is indeed expected to be finite in three dimensions, except when the field lines form an Abrikosov flux lattice [2].

VI. RENORMALIZATION-GROUP ANALYSIS OF THE DILUTE LIMIT

The analysis in the previous sections applies when the chains are dense and entangled. To treat the dilute limit, we perturb about the limit in which $\langle\psi\rangle\approx 0$. To this end, we again consider the (coherent-state) functional-integral representation of the partition function

$$Z_{\rm gr}=\int\mathcal{D}\psi\,\mathcal{D}\psi^*\mathcal{D}\,\delta\vec{n}\exp(-S[\psi,\psi^*,\delta\vec{n}]) \tag{6.1}$$

and break the action into three parts,

$$\begin{aligned}S[\psi,\psi^*,\delta\vec{n}]=&\int d^dr\int dz[\psi^*(\partial_z-D\nabla_\perp^2-\bar{\mu})\psi+v|\psi|^4]\\&+\frac{\lambda}{2}\int d^dr\int dz\,\delta\vec{n}\cdot(\psi^*\nabla_\perp\psi-\psi\nabla_\perp\psi^*)\\&+F_n[\delta\vec{n}]/k_BT\ .\end{aligned} \tag{6.2}$$

This form of the action is just (3.8), specialized to the case $\bar{v}(\vec{r})=v\delta^d(\vec{r})$ and with a new parameter λ to help organize perturbation theory in the coupling between the polymer and nematic degrees of freedom. As in Ref. [1], we impose a cutoff Λ on the perpendicular wave vectors $\vec{q}_\perp$, of the order of the inverse range of the interaction. For now we neglect the possibility of free ends and do not introduce a source term. It is convenient to consider $(d+1)$-dimensional directed polymers with d directions perpendicular to the average direction. We take the limit $d=2$ at the end of the calculation.

We can now attempt to expand quantities of physical interest in the nonlinear couplings v and λ. Consider, for example, the propagator

$$G(\vec{r},z)=\langle\psi(\vec{r},z)\psi^*(\vec{0},0)\rangle \tag{6.3}$$

or, in Fourier space

$$G(\vec{q}_\perp,q_z)=\langle|\psi(\vec{q}_\perp,q_z)|^2\rangle \ . \tag{6.4}$$

This can be written as

$$G(\vec{q}_\perp,q_z)=\frac{1}{-iq_z+Dq_\perp^2-\bar{\mu}+\Sigma(\vec{q}_\perp,q_z)} \ , \tag{6.5}$$

where, to lowest, nontrivial order in v and λ, the self-energy graphs shown in Fig. 12 lead to

$$\Sigma(\vec{q}_\perp,q_z)=-\frac{1}{2\pi}\int dk_z\frac{1}{(2\pi)^d}\int d^dk_\perp\left[\frac{\lambda^2}{4}\frac{(2q_\perp-k_\perp)^i(2q_\perp-k_\perp)^j}{-i(q_z-k_z)+D(\vec{q}_\perp-\vec{k}_\perp)^2-\bar{\mu}}\times\left[\frac{k_\perp^ik_\perp^j/k_\perp^2}{K_1k_\perp^2+K_3k_z^2}+\frac{\delta^{ij}-k_\perp^ik_\perp^j/k_\perp^2}{K_2k_\perp^2+K_3k_z^2}\right]-2v\frac{1}{-ik_z+Dk_\perp^2-\bar{\mu}}\right] . \tag{6.6}$$

The first term comes from the nematic-matrix–polymer interaction, while the second term arises from the polymer-polymer interaction. This self-interaction of a single polymer is not present in the original microscopic model (1.2) and arises here because of the nonuniversal cutoff dependence (in q_z) of the Feynman path integrals and their representation as a coherent-state functional integral [1]. We interpret the integral over q_z in such a way that its imaginary part vanishes. The real part is well defined and simply gives a constant renormalization of the chemical potential. After integrating over k_z and evaluating (6.6) in the zero-frequency, long-wavelength regime we find

$$\Sigma(\vec{q}_\perp,0)=-\frac{\lambda^2}{4}\frac{1}{(2\pi)^d}\int d^dk_\perp\frac{k_\perp^2+(4/d)q_\perp^2}{2\sqrt{K_1K_3}|k_\perp|(\sqrt{K_1/K_3}|k_\perp|+Dk_\perp^2-\bar{\mu})}$$
$$-\frac{\lambda^2}{4}\frac{1}{(2\pi)^d}\int d^dk_\perp\frac{4(1-1/d)q_\perp^2}{2\sqrt{K_2K_3}|k_\perp|(\sqrt{K_2/K_3}|k_\perp|+Dk_\perp^2-\bar{\mu})}+v\frac{1}{(2\pi)^d}\int d^dk_\perp \ . \tag{6.7}$$

Although the correction to $\bar{\mu}$ in (6.5) is well behaved, the renormalization of D represented by the coefficient of $q_\perp^2$ diverges for $d\leq 2$, when $\bar{\mu}\approx 0$. This infrared divergence suggests that renormalization-group techniques by employed to study the system for $d\leq 2$. Our approach follows [48], which is a variation of the dynamic renormalization-group method of Ref. [49]. First we integrate out a momentum shell in $k_\perp$ from Λe^{-l} to Λ, but integrate freely over k_z. We then rescale our variables so that the ultraviolet cutoff is held fixed. After rescaling ψ and $\delta\vec{n}$ accordingly, we are left with the same theory but with different coupling constants. When this procedure is iterated, λ and v are driven toward a fixed point that describes the universal long-wavelength behavior in the dilute limit.

A. Momentum-shell integration

We must first integrate out the transverse momentum in the range $\lambda e^{-l}<q_\perp<\Lambda$. This can be done straightforwardly by expanding the functional integral (6.1) in v and λ. The expansion can be represented diagrammatically as in Fig. 12. Care must be taken to account for all possible contractions of the operators in the expansion. The symmetry factors can be found in the usual way for Wick expansions. It is important to note that diagrams renormalize the remaining low-momentum modes and are not simply expectation values. The diagrammatic rules may be summarized as follows.

(i) For each line, assign a momentum k_i while conserving energy and momentum at the vertices.

(ii) For each polymer line include a factor of $1/(-ik_z+Dk_\perp^2-\bar{\mu})$. The sign of k_z is determined by the direction of the line.

(iii) For each nematic line include a factor of

$$\frac{k_\perp^ik_\perp^j/k_\perp^2}{K_1k_\perp^2+K_3k_z^2}+\frac{\delta^{ij}-k_\perp^ik_\perp^j/k_\perp^2}{K_2k_\perp^2+K_3k_z^2} \ .$$

(iv) If a vertex joins four polymer lines, include a factor of $2v$.

(v) If a vertex joins two polymer lines and one nematic line, include a factor of $\lambda/2$ and the sum of the incoming and outgoing polymer momentum.

(vi) Divide by the symmetry factor. The symmetry factor is the product of the number of ways of permuting the vertices and the number of ways of permuting the lines while keeping the contractions the same.

(vii) Integrate over all momenta q_z, but only integrate the transverse momenta from Λe^{-l} to Λ.

Upon carrying out this procedure, we arrive at the following relations for the intermediate values of the coupling constants:

$$D'=D\left[1+\frac{\lambda^2}{D}\left[\frac{K_1(d-1)+K_2}{K_1K_2}\right]\times\frac{A_d\Lambda^{d-2}}{2d}\frac{(1-e^{-(d-2)l}}{d-2}\right] , \tag{6.8a}$$

$$\lambda'=\lambda\ , \tag{6.8b}$$

$$v'=v-\left[\frac{v^2}{4D}-\frac{\lambda^2 v}{4K_1 D}+\frac{\lambda^4}{16K_1^2 D}\right]\times\frac{A_d\Lambda^{d-2}(1-e^{-(d-2)l})}{d-2}\ , \tag{6.8c}$$

$$K_i'=K_i\ ,\quad i=1,2,3\ , \tag{6.8d}$$

$$\bar{\mu}'=\bar{\mu}-\left[\frac{v}{D}+\frac{\lambda^2}{8K_1 D}\right]\frac{A_d D\Lambda^d}{d}(1-e^{-dl})\ , \tag{6.8e}$$

where $A_d=2/[\Gamma(d/2)(4\pi)^{d/2}]$. In evaluating the integrals we have ignored term of two types. If a term diverges as $l\to\infty$ in a smaller dimension than the most divergent term, it is irrelevant by power counting. Further, there are terms that appear to diverge in a higher dimension, but they are all higher order in the external momenta. When we rescale we must rescale these momenta. Doing so will render these terms irrelevant in the renormalized and rescaled theory. The intermediate values of D, $\bar{\mu}$, and the Frank constants reflect all the contributions to them at one-loop order, while the expressions for λ and v represent only the most relevant contribution to their values.

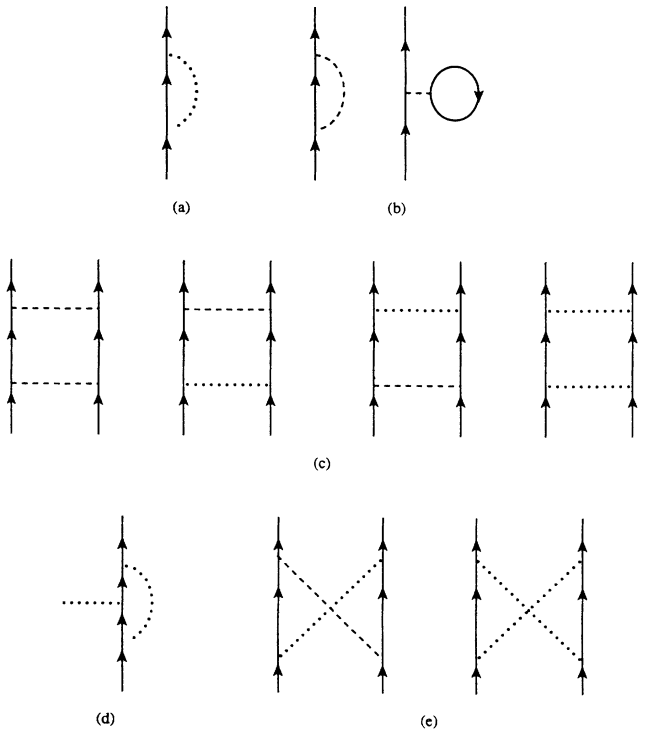

FIG. 12. Lowest-order contributions to the perturbation expansion used in calculating corrections to the zeroth-order parameters in the theory. Graphs that are identically 0 due to the retarded nature of the polymer propagator are not included. In this case, the internal lines are only integrated over a small spatial momentum shell $e^{-l}<q_\perp<1$, but are integrated over all timelike momenta q_z. (a) and (b) The contributions to the self-energy of the polymer propagator. The contributions (b) are just constants that we must absorb into a redefinition of the chemical potential $\bar{\mu}$. (c) Graphs that renormalize the four-point coupling v. (d) The corrections to the vertex between the nematic director $\delta\vec{n}$ and the polymers. (e) Two graphs that contribute to the four-point coupling but do not vanish identically. However, their contribution is irrelevant by power counting.

These intermediate coupling constants have not yet been rescaled. We rescale lengths by $L'=Le^{-l}$ and times by $T'=Te^{-\int_0^l\gamma(l')dl'}$. We now set $q_\perp'=q_\perp e^{l}$ and $q_z'=q_z e^{\int_0^l\gamma(l')dl'}$, where the function $\gamma(l)$ is to be determined. The dimension of $\psi(\vec{r},t)$ is just $(L^d)^{-1/2}$. Note that even when we rescale, $\psi(\vec{r},t)$ will rescale trivially because it has no time dimensions. $\psi(\vec{r},t)$ has no anomalous dimension in our renormalization scheme, to leading order in $\epsilon=2-d$.

When doing the first-momentum-shell integration, the coupling constants were independent of length scale. However, they then acquire a momentum dependence because we have absorbed the large momentum effects into them. The correct renormalized theory is a coupled set of integral equations where the coupling constants are taken to be scale dependent. An alternative, but equivalent approach is to integrate over a small momentum range where the coupling constants are approximately fixed and then repeat the entire calculation iteratively. This leads to the usual differential renormalization-group equations.

B. Recursion relations

We now choose an infinitesimal momentum shell $e^{-\delta}$ and take the limit $\delta\to 0$. This leads to differential renormalization-group equations that can be integrated to produce the couplings appropriate for a cutoff $q_\perp<\Lambda e^{-l}$. We use units such that $\Lambda=1$ in the following. The differential recursion relations are

$$\frac{dD(l)}{dl}=D\left[-2+\gamma+\frac{\lambda^2}{D}\frac{K_1(d-1)+K_2}{K_1K_2}\frac{A_d}{2d}\right]\ , \tag{6.9a}$$

$$\frac{d\lambda(l)}{dl}=\lambda(-1+\gamma)\ , \tag{6.9b}$$

$$\frac{dv(l)}{dl}=v\left[-d+\gamma-\frac{v}{2D}A_d+\frac{\lambda^2}{K_1 4D}A_d\right]-\frac{\lambda^4}{K_1^2 32D}A_d\ , \tag{6.9c}$$

$$\frac{dK_1(l)}{dl}=K_1(d-2+\gamma)\ , \tag{6.9d}$$

$$\frac{dK_2(l)}{dl}=K_2(d-2+\gamma)\ , \tag{6.9e}$$

$$\frac{dK_3(l)}{dl}=K_3(d-\gamma)\ , \tag{6.9f}$$

$$\frac{d\bar{\mu}(l)}{dl}=\bar{\mu}\gamma-\left[\frac{v}{D}+\frac{\lambda^2}{8K_1D}\right]A_d D\ . \tag{6.9g}$$

It is convenient to chose $\gamma(l)$ so that the renormalized, rescaled D remains fixed at its initial value. By examin-

ing (6.9) we can see that there are three dimensionless coupling constants which come into this theory:

$$\bar{\lambda}_1=\lambda[K_1(d-1)+K_2]^{1/2}(K_1K_2D)^{-1/2},$$

$$\bar{\lambda}_2=\lambda(K_1D)^{-1/2}$$

and

$$\bar{v}=v/D .$$

The quantity $\bar{\lambda}_1$ controls the coupling between the tangent field of the polymers and the nematic matrix. The coupling $\bar{\lambda}_2$ represents the interactions between density fluctuations in the polymers and the nematic. Note that none of the dimensionless couplings depend on the bend Frank constant K_3. For noninteracting polymers $q_z\sim q_\perp^2$. Thus we expect that the term $\frac{1}{2}K_3q_z^2|\delta\vec{n}|^2\sim q_\perp^4$ and will be suppressed at very long wavelengths. This is why the bend elastic constant does not couple to the theory at this order, though presumably it will at higher order.

The result that the geometric mean of the splay and twist Frank constants comes into $\bar{\lambda}_1$ is not unexpected. In Ref. [8] it is shown that the effective rigidity of a polymer in a nematic matrix is the harmonic mean of its original rigidity and the induced rigidity from the matrix. We can understand the meaning of this harmonic mean by considering the following static example of a single polymer. If the polymer deviates away from the $\hat{z}$ direction, the nematic matrix can relieve the stress in the *same* time slice by a twist, a splay, or by a combination of the two. In d dimensions, there are $d-1$ twist directions and only 1 splay direction. In the static limit, where $q_z=0$, the matrix bends back to its preferred direction over the transverse plane, whether the relief is through a twist or a bend. This allows us to estimate the nematic energy cost in disturbing the polymer,

$$\delta F\propto\alpha^2K_1+(d-1)\left[\frac{1-\alpha}{d-1}\right]^2K_2 , \tag{6.10}$$

where $0\le\alpha\le1$ measures the fraction of the distortion relieved by a splay mode, and $(1-\alpha)/(d-1)$ is the fraction of the distortion carried by each of the equivalent twist modes. Minimizing the energy with respect to α, we find that

$$\delta F\propto\alpha^2\left[\frac{K_1K_2}{K_1(d-1)+K_2}\right], \tag{6.11}$$

showing that the coupling to tangent fluctuations is given by $\bar{\lambda}_1$.

Finally, $\bar{\lambda}_2$ is the coupling between the polymer and the splay degrees of freedom of the nematic matrix. As we have seen, this coupling comes about through density fluctuations of the polymers. The effect of the nematic matrix is to create an attraction between polymers, not unlike the van der Waals attraction between neutral bodies.

C. Fixed points and flows

Our theory is described by the full space of all the coupling constants. We can describe the flow of the theory towards a stable theory by analyzing its fixed-point structure in this space. The behavior of the Frank constants is trivial, amounting to a mere rescaling. We assume, moreover, that the chemical potential has been adjusted to the critical point that describes the critical point of the theory [1].

We will analyze the flow in terms of the variables described above, namely $\bar{v}$, $\bar{\lambda}_2$, and $\bar{\lambda}_1$ near $d=2$. From (6.9) we find

$$\frac{d\bar{v}}{dl}=\bar{v}\left[\epsilon-\frac{\bar{v}}{4\pi}+(\bar{\lambda}_2^2-\bar{\lambda}_1^2)\frac{1}{8\pi}\right]-\frac{\bar{\lambda}_2^4}{64\pi} . \tag{6.12a}$$

$$\frac{d\bar{\lambda}_1}{dl}=\bar{\lambda}_1\left[\frac{\epsilon}{2}-\frac{\bar{\lambda}_1^2}{16\pi}\right], \tag{6.12b}$$

$$\frac{d\bar{\lambda}_2}{dl}=\bar{\lambda}_2\left[\frac{\epsilon}{2}-\frac{\bar{\lambda}_1^2}{16\pi}\right] . \tag{6.12c}$$

Note that $\bar{\lambda}_2$ is slaved to $\bar{\lambda}_1$ in the sense that their ratio is independent of l. If we let $u=\bar{v}-(1/4)\bar{\lambda}_2^2$, the recursion relation for $u(l)$ depends only on $\bar{\lambda}_1^2$

$$\frac{du}{dl}=u\left[\epsilon-\frac{\bar{\lambda}_1^2}{8\pi}-\frac{u}{4\pi}\right], \tag{6.13}$$

so that it suffices to consider flows in the space of $u(l)$ and $\bar{\lambda}_1^2(l)$. The subspace $\bar{\lambda}_1^2=0$ is the theory considered by Nelson and Seung [1] for flux lines, while the subspace $u=0$ is the noninteracting theory considered by de Gennes [8]. By examining the flow to the fixed point, we can decide which theory dominates in the long-wavelength limit.

Since the dimension of interest is $d=2$, we discuss the flows for $\epsilon=0$. In this case we can solve (6.12b) for $\bar{\lambda}_1^2(l)$,

$$\bar{\lambda}_1^2(l)=\frac{\bar{\lambda}_1^2(0)}{\left[1+\frac{\bar{\lambda}_1^2(0)}{8\pi}l\right]}\underset{l\to\infty}{\sim}\frac{8\pi}{l} \tag{6.14}$$

and then solve for u,

$$u(l)=\frac{u(0)}{\left[1+\frac{\bar{\lambda}_1^2(0)}{8\pi}l\right]\left[1+\frac{2u(0)}{\bar{\lambda}_1^2(0)}\ln\left[1+\frac{\bar{\lambda}_1^2}{8\pi}l\right]\right]}$$

$$\underset{l\to\infty}{\sim}\frac{4\pi}{l\ln l} \tag{6.15}$$

if $\bar{\lambda}_1(0)\neq0$. If $\bar{\lambda}_1(0)=0$, $u(l)$ is given asymptotically by $4\pi/l$, in agreement with the results in Ref. [1]. The flows are illustrated in Fig. 13.

If $u_0>0$, the flows go to the origin in the $(\bar{\lambda}_1^2,u)$ plane. For nonzero $\bar{\lambda}_1^2(0)$, they come into the origin tangent to the $\bar{\lambda}_1^2$ axis. This means that the logarithms that de Gennes discussed for a *single* polymer dominate the logarithms associated with interpolymer interactions. If, on

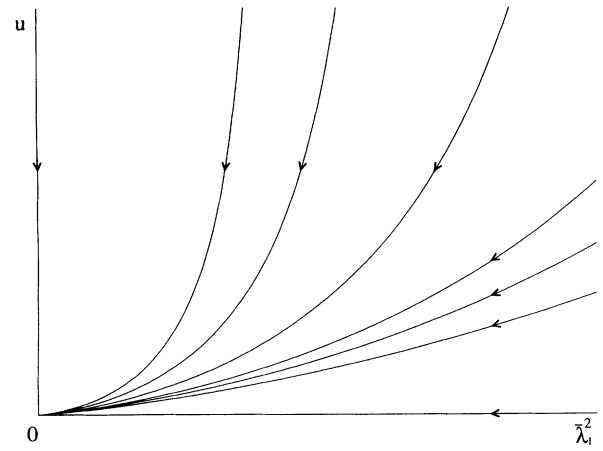

FIG. 13. Fixed-point flow in three dimensions ($d=2$). We show u, the effective hard-core repulsion and $\bar{\lambda}_1^2$. The flows come into the origin tangent to the $\bar{\lambda}_1^2$ axis. If $u_0<0$, then the flow in u_0 runs off to large negative values, and the system will go through a gas-liquid phase transition.

the other hand, $u_0<0$, the flows will still run to $\bar{\lambda}_1^2=0$, but u will run off to $-\infty$. Since u is the coefficient of ρ^2 in the hydrodynamic theory, this flow will push the system through a gas-liquid phase transition, since presumably there are higher-order terms in both the hydrodynamic and boson language, corresponding to many-polymer interactions.

Finally, we can calculate the logarithmic corrections to the wandering of a single polymer in the dilute limit,

$$\langle |\vec{r}(L)-\vec{r}(0)|^2\rangle = \frac{\int d^2r\, r^2\langle \psi(\vec{r},L)\psi^*(\vec{0},0)\rangle}{\int d^2r\langle \psi(\vec{r},L)\psi^*(\vec{0},0)\rangle} . \tag{6.16}$$

In order to do this, we observe that

$$\langle \psi(\vec{r},z)\psi^*(\vec{0},0)\rangle_{l=0} = e^{dl}\langle \psi(e^{-l}\vec{r}, e^{-\int_0^l \gamma(l')dl'}z) \times \psi^*(\vec{0},0)\rangle_l . \tag{6.17}$$

We have chosen $\gamma(l)$ so that D will remain fixed at every scale, i.e., $\gamma(l)=2-\bar{\lambda}_1^2(l)/8\pi$. This choice is arbitrary and, of course, does not affect the expressions for physical quantities.

We now choose l^* such that $z'=e^{-\int_0^{l^*}\gamma(l')dl'}z=a_0$, where a_0 is the persistence length of a single, *directed* polymer. As $z\to\infty, l^*$ becomes large enough so that we have flowed very close to the stable fixed point in Fig. 13. Since λ_1, $\bar{\lambda}_2$, and $\bar{v}$ are small near this fixed point, we can simply use the zeroth-order term in perturbation theory to calculate the two-point function. We have

$$\begin{aligned}\langle |\vec{r}(z)-\vec{r}(0)|^2\rangle_{l=0} &= e^{2l^*}\langle |\vec{r}'(z')-\vec{r}'(0)|^2\rangle_{l=l^*} \\ &= e^{2l^*}\frac{\int d^2r'(r')^2\langle \psi(\vec{r}',z')\psi^*(\vec{0},0)\rangle_{l=l^*}}{\int d^2r'\langle \psi(\vec{r}',z')\psi^*(\vec{0},0)\rangle_{l=l^*}} \\ &= 2dDe^{2l^*}z' = 2dDze^{\int_0^{l^*}[2-\gamma(l')]dl'} .\end{aligned} \tag{6.18}$$

Substituting $\bar{\lambda}_1^2(l)/8\pi$ for $2-\gamma(l)$, we can integrate (6.14) when $d=2$ and find

$$\langle |\vec{r}(z)-\vec{r}(0)|^2\rangle_{l=0} = 4Dz\left[1+\frac{\bar{\lambda}_1^2(0)}{8\pi}l^*\right] . \tag{6.19}$$

Our choice of l^* amounts to choosing $l^*\approx\frac{1}{2}\ln(z/a_0)$. Substituting this into (6.19) and writing λ_1 in terms of the original couplings (with $\lambda=1$, as it was originally)

$$\langle |\vec{r}(z)-\vec{r}(0)|^2\rangle = 4Dz+\frac{K_1+K_2}{4\pi(K_1K_2)}z\ln\left[\frac{z}{a_0}\right] \tag{6.20}$$

again resulting in a logarithmic correction to wandering. Comparison with de Gennes's result (2.7) shows that the logarithmic correction to wandering is only half as large as would be predicted by the simple argument in Sec. II.

The correlation $\langle \psi(\vec{r},z)\psi^*(\vec{0},0)\rangle$ is the probability distribution for the wandering of a *single* polymer only in the dilute limit. This correlation function represents inserting a polymer at $(\vec{0},0)$ and removing a polymer at $(\vec{r},z)$, but there is no constraint that it be the same polymer. However, if the system is sufficiently dilute, the likelihood of polymers swapping their heads and tails is small. In the above derivation, we halted our renormalization-group iteration when $z\sim a_0$. However, we can also stop iterating when the polymer density ρ_0 becomes of the order of Λ^2. Since Λ^{-1} is of the order of monomer thickness, we can then apply the hydrodynamic theory of Sec. V.

For fixed z, we can always make the system dilute enough so that as we follow the renormalization-group trajectory $z(l)\sim a_0$ *before* $\rho(l)\sim\Lambda^2$, where $z(l)=ze^{-\int_0^l\gamma(l')dl'}z$ and $\rho(l)=e^{2l}\rho_0$. In this regime the wandering is given by (6.20). However, as the density increases, we come to a point where $\rho(l)\sim\Lambda^2$ *before* $z(l)\sim a_0$. Now we must choose l^* so that $\rho(l^*)\Lambda^2=1$. In this case (6.20) will cross over to

$$\langle |\vec{r}(z)-\vec{r}(0)|^2\rangle = 4Dz+\frac{K_1+K_2}{4\pi(K_1K_2)}z\ln\left[\frac{1}{\rho_0\Lambda^2}\right] . \tag{6.21}$$

This result will hold when $z/a_0>1/\rho_0\Lambda^2$. In this very

long polymer regime, the interpolymer interactions destroy the logarithmic correction to wandering. Each time the polymers wander into each other, the random walk is reset, and thus the logarithm does not build up along their length.

VII. EFFECTS OF HAIRPINS

In the preceding sections we consider polymers without hairpin configurations. As in Sec. II C, we can account for hairpins by adding a term to the action (6.2), namely

$$S \to S - \frac{w}{2} \int dz\, d^2r [\psi^2 + (\psi^*)^2] \,. \tag{7.1}$$

The coupling $w \propto \exp(-\epsilon_h / k_B T)$, where the hairpin energy ϵ_h is related to the coupling constants in (1.2) by $\epsilon_h = O(\sqrt{g\kappa})$—see Sec. II C. Upon repeating the analysis of Sec. III B, we see that these terms create and destroy *pairs* of polymer lines and so add hairpins to the theory.

Upon carrying out perturbation theory in v and w, we find that unphysical diagrams appear in our theory. By allowing hairpins, we now also include loops of interacting polymers as in Fig. 14(a). However, following de Gennes [50], we can eliminate closed loops of polymers by replicating $\psi(\vec{r},z)$ M times, and then taking the limit $M \to 0$. This could also have been done in our earlier analysis, although it is unnecessary, due to the retarded nature of the propagators. In the theory without hairpins but with free ends, one might think that the free ends generate an effective hairpin term as in Fig. 14(b). However, the effective hairpin strength is $O(h^2)$ and makes good physical sense. With free ends present, a long polymer may interact with two short polymers, simulating the effect of an intervening closed-loop polymer. We must be certain that taking $M \to 0$ preserves these graphs. Consider the action of M polymer fields coupled to a source (without explicit hairpins),

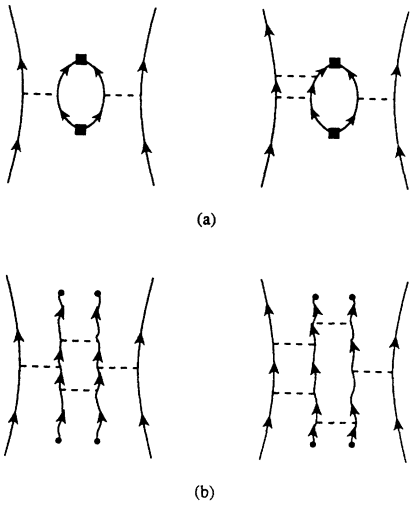

FIG. 14. In these graphs, we represent a hairpin insertion by a solid square and the insertion of a free end by a solid circle. (a) Diagrams that involve closed loops of polymers interacting with physical polymers. These graphs do not factor into a physical part and an unphysical part. (b) Graphs appearing in a theory with free ends that appear to involve closed loops of polymers, but instead are interacting with two or more short polymers. These graphs are indeed physical.

$$S = \sum_{\alpha=1}^{M} \int dz\, d^2r \left[\psi_\alpha^* (\partial_z - D\nabla_\perp^2 - \bar{\mu}) \psi_\alpha + \frac{v}{2} \sum_{\beta=1}^{M} \psi_\alpha^* \psi_\beta^* \psi_\alpha \psi_\beta + \frac{\lambda}{2} \delta\vec{n} \cdot (\psi_\alpha^* \nabla_\perp \psi_\alpha - \psi_\alpha \nabla_\perp \psi_\alpha^*) - h_\alpha (\psi_\alpha^* + \psi_\alpha) \right] + \frac{F_n[\delta\vec{n}]}{k_B T} \,. \tag{7.2}$$

By changing the replica basis, we can choose to only allow the $\alpha = 1$ direction to have a source term. Because of the preferential status of this direction, the effective closed loops will be $O(1)$, as opposed to $O(M)$ in the case of real closed loops. Thus taking $M \to 0$ will not alter the results found earlier for free ends.

In the dense phase, hairpins lead to effects very similar to those discussed for free ends in Sec. IV. To see how hairpins affect the transition near $\bar{\mu} = 0$, we first set $\psi \equiv (\psi_1 + i\psi_2)/\sqrt{2}$, and note that the action takes the form

$$S = \frac{F_n[\delta\vec{n}]}{k_B T} + \int dz\, d^2r \left[i\psi_{\alpha 1} \partial_z \psi_{\alpha 2} + \tfrac{1}{2}\psi_{\alpha 1}[-D\nabla_\perp^2 - (\bar{\mu} - w)]\psi_{\alpha 1} + \tfrac{1}{2}\psi_{\alpha 2}[-D\nabla_\perp^2 - (\bar{\mu} + w)]\psi_{\alpha 2} \right.$$
$$\left. + \frac{v}{8}(\psi_{\alpha 1}^2 + \psi_{\alpha 2}^2)(\psi_{\beta 1}^2 + \psi_{\beta 2}^2) + i\frac{\lambda}{2} \delta\vec{n} \cdot (\psi_{\alpha 1} \nabla_\perp \psi_{\alpha 2} - \psi_{\alpha 2} \nabla_\perp \psi_{\alpha 1}) \right] , \tag{7.3}$$

where we have followed the usual summation convention. Recursion relations can be constructed as before for finite M, resulting in

$$\frac{d\bar{\mu}(l)}{dl} = \bar{\mu}\gamma - \left[\frac{\bar{v}}{2\pi}(M+1) + \frac{\bar{\lambda}_2^2}{8\pi} \right] D \,, \tag{7.4a}$$

$$\frac{dw(l)}{dl} = w \left[\gamma - \frac{u}{4\pi} \right] , \tag{7.4b}$$

where $u = v - \bar{\lambda}_2^2/4$ was defined in the previous section. The recursion relations for the other variables remain the same as in (6.9a)–(6.9f). Upon taking $M \to 0$ we see that

only the recursion relation for μ is different from (6.9g) and that (since $\gamma=2$) w is a strongly relevant perturbation. Although $\bar{\mu}$ has a different recursion relation, this has no effect on the universal long-wavelength properties. The $M\to 0$ limit amounts to removing the second graph in Fig. 7(c), while keeping the first graph. As before, the surviving graph can be absorbed into a change in the chemical potential.

Suppose our system is very dilute, i.e., $\bar{\mu}\lesssim 0$ and $w>0$, so that ψ_2 will condense. We can follow $\bar{\mu}+w$ via the recursion relations (7.4). The coupling $\bar{\mu}+w$ grows rapidly under iteration, until it becomes large enough so that we can integrate out the massive modes corresponding to $\{\psi_{\alpha 2}\}$. The resulting theory involves only $\psi_{\alpha 1}$ and $\delta\vec{n}$,

$$S_{\rm eff}=\int dz\, d^2r_\perp \left[\tfrac{1}{2}(\partial_z\psi_{\alpha 1})^2+\frac{D}{2}(\nabla_\perp\psi_{\alpha 1})^2-\frac{\bar{\mu}_1}{2}\psi_{\alpha 1}^2 +v\psi_{\alpha 1}^2\psi_{\beta 1}^2+\frac{\lambda^2}{4}(\nabla_\perp\psi_{\alpha 1}\cdot\delta\vec{n})^2 +\lambda(\nabla_\perp\psi_{\alpha 1}\cdot\delta\vec{n})\partial_z\psi_{\alpha 1}\right]+\frac{F_n[\delta\vec{n}]}{k_BT} \tag{7.5}$$

with $\bar{\mu}_1=\bar{\mu}-w$. We now have a theory in which directed propagators are replaced by merely anisotropic gradient couplings—the meandering in the parallel direction scales just as the meandering in the perpendicular direction with different proportionality constants. The couplings shown in (7.5) only serve as a caricature of those found in the theory—they will be changed by numerical factors depending on at which point we integrate out ψ_2. As we go through the dilute-dense phase transition by letting $\bar{\mu}_1$ change sign, the theory describes a quasi-isotropic polymer melt with the self-avoidance in the limit $M\to 0$ [39,50].

The dilute limit of directed polymer melts *without* hairpins is described by an XY-like critical point (with a diffusive propagator), as indicated by Fig. 8. The change in this phase transition induced by hairpins can be summarized by considering the mean-field diagram (see Fig. 15) associated with the polynomial part of (7.3). We imagine holding v and w fixed and varying the chemical potential $\bar{\mu}$ in the plane of $r_1=-\bar{\mu}+w$ and $r_2=-\bar{\mu}-w$. When $w=0$, the critical point at $r_1=r_2=0$ is just that considered in Fig. 8. When $w\neq 0$, however, the trajectory as $\bar{\mu}$ varies passes through one of the Ising-like critical lines (with a quasisotropic effective propagator, see Eq. 7.5) on the r_1 and r_2 axes. In a similar fashion, the line describing the XY-like symmetry of the dense phase for $r_1=r_2<0$ becomes unstable to Ising-like dense phases when $w=0$.

The above discussion ignores the coupling to the nematic field. This theory is similar to the compressible Ising model [51] though the marginal operator present in that theory is not present in ours. This is guaranteed by the underlying nematic symmetry of our theory. Note that the original field theory is invariant under $\delta\vec{n}\to-\delta\vec{n}$, $\psi\leftrightarrow\psi^*$, and $z\to -z$. This prevents a term such as $(\nabla_\perp\cdot\delta\vec{n})\psi_1^2$, the usual coupling of the Ising model to an underlying elastic lattice. The couplings that do appear do not affect the above arguments, and we are left with an M component Ising model as $M\to 0$, reproducing de Gennes's theory of isotropic polymers. Note that the upper critical dimension of this Ising-like transition is $d_c=4$, as opposed to the result $d_c=2+1=3$ appropriate when $w=0$.

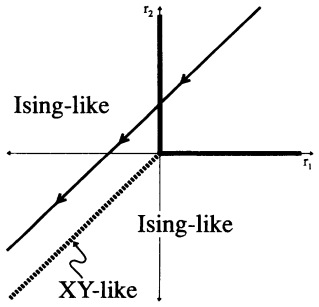

FIG. 15. Trajectory with varying $\bar{\mu}$ through the r_1-r_2 plane, where $r_1=-\bar{\mu}+w$ and $r_2=-\bar{\mu}-w$. For $w\neq 0$, the transition from the dilute limit corresponds to an Ising-like phase transition. The line $r_1=r_2<0$ corresponds to an XY-like phase.

ACKNOWLEDGMENTS

It is a pleasure to acknowledge helpful conversations with L. Balents, T. Hwa, M. Goulian, and R. B. Meyer during the course of this investigation. One of us (R.D.K.) would like to acknowledge financial support from the National Science Foundation. This work was supported by the National Science Foundation, through Grant No. DMR91-15491 and through the Harvard Materials Research Laboratory.

APPENDIX A: CONSEQUENCES OF ROTATIONAL INVARIANCE

The full rotationally invariant coupling between the nematic and the polymer is given by

$$F=g\int ds\left[1-\left[\frac{d\mathbf{R}(s)}{ds}\cdot\mathbf{n}\right]^2\right]+F_n[\mathbf{n}]\ , \tag{A1}$$

where s is the arclength along the polymer. We now consider the following transformations of our fields (leaving all other fields the same):

$$\begin{aligned} &n_x\to n_x+v_x\ ,\quad n_y\to n_y+v_y\\ &R_z(s)\to R_z(s)-v_xR_x(s)-v_yR_y(s)\ , \end{aligned} \tag{A2}$$

where $\vec{v}=(v_x,v_y)$ is a constant vector in the plane perpendicular to $\hat{z}$. It is easy to check that (A1) is invariant under these transformations if H, the magnetic field, is 0. In terms of the small deviations defined in Sec. II, this transformation, to linear order in $\mathbf{v}$ and the fields, is

$$\delta\vec{n}'(\vec{r}'(z'),z')=\delta\vec{n}(\vec{r}(z),z)+\vec{v} \tag{A3}$$

and

$$\frac{d\vec{r}'(z')}{dz'}=\frac{d\vec{r}(z)}{dz} \tag{A4}$$

and thus to linear order in $\vec{v}$

$$F' = F + g \int dz\, \vec{v} \cdot \left[\frac{d\vec{r}(z)}{dz} - \delta\vec{n}(\vec{r}(z), z) \right] . \tag{A5}$$

However, we may absorb the shift in $\delta\vec{n}$ into a redefinition of the field, so as to eliminate the effect of the transformation and find that F is invariant under (A2).

Returning now to the coherent-state field theory (3.8), we find that it must be invariant under

$$\begin{aligned} \delta\vec{n}'(\vec{r}', z') &= \delta\vec{n}(\vec{r}, z) + \vec{v} , \\ \partial_z' &= \partial_z - \vec{v} \cdot \nabla_\perp . \end{aligned} \tag{A6}$$

We now change the coefficient of $\psi^* \partial_z \psi$ from 1 to some constant value α. The transformations lead us to

$$\begin{aligned} S_\alpha'[(\psi')^*, \psi', \delta\vec{n}'] &= S_\alpha[\psi^*, \psi, \delta\vec{n}] + \vec{v} \cdot \int dz\, d^2r (-\alpha) \psi^s{}_* \nabla_\perp \psi + \tfrac{1}{2}(\psi^* \nabla_\perp \psi - \psi \nabla_\perp \psi^*) \\ &= S_\alpha[\psi^*, \psi, \delta\vec{n}] + (1-\alpha) \int dz\, d^2r\, \vec{v} \cdot \psi^* \nabla_\perp \psi . \end{aligned} \tag{A7}$$

Thus S will only be independent of $\mathbf{v}$ if $\alpha = 1$.

APPENDIX B: DERIVATION OF HYDRODYNAMICS

In fact, the hydrodynamic theories described in Sec. IV can be derived from the more microscopic boson theory [52]. To this end, we begin with (4.3), taking $h = 0$ to start,

$$S_p = \int dz\, d^2r \left[\frac{D(\nabla_\perp \rho)^2}{4\rho} + D\rho(\nabla_\perp \theta)^2 + i\rho \partial_z \theta + i\rho \nabla_\perp \theta \cdot \delta\vec{n} - \bar{\mu}\rho + \frac{v}{2}\rho^2 \right] . \tag{B1}$$

We now introduce a vector field $\vec{P}$, via a Hubbard-Stratonovich transformation, in order to eliminate the $D\rho(\nabla_\perp \theta)^2$ term in (B1). We now have

$$Z_p = \int \mathcal{D}\vec{P}\, \mathcal{D}\rho\, \mathcal{D}\theta\, e^{-S_p'} \tag{B2}$$

with

$$S_p' = \int dz\, d^2r \left[\frac{D(\nabla_\perp \rho)^2}{4\rho} + i\rho \partial_z \theta + i\rho \nabla_\perp \theta \cdot \delta\vec{n} - \bar{\mu}\rho + \frac{v}{2}\rho^2 + D\rho \vec{P}^2 + 2iD\rho \vec{P} \cdot \nabla_\perp \theta \right] . \tag{B3}$$

If we integrate out $\vec{P}$ we return to the original action S_p. However, we can now integrate over θ. Since it appears but linearly in S_p', its integration results in a δ-functional

$$Z = \int \mathcal{D}\vec{P}\, \mathcal{D}\rho\, e^{-S_H} \delta[\partial_z \rho + \nabla_\perp \cdot (\rho \delta\vec{n} + 2D\vec{P})] , \tag{B4}$$

where

$$S_H = \int dz\, d^2r \left[D\rho \vec{P}^2 + \frac{D(\nabla_\perp \rho)^2}{4\rho} - \bar{\mu}\rho + \frac{v}{2}\rho^2 \right] . \tag{B5}$$

Thus we have traded interactions between θ and $\delta\vec{n}$ for a constraint relating ρ, $\vec{P}$, and $\delta\vec{n}$. We must now identify the physical meaning of $\vec{P}$. In the case $\delta\vec{n} = 0$, the constraint in (B4) becomes

$$\partial_z \rho + \nabla_\perp \cdot (2D\rho\vec{P}) = 0 , \tag{B6}$$

which suggests that $2D\rho\vec{P}$ is the "tangent" field introduced in Sec. V. However with the nematic field included, we would have

$$\partial_z \rho + \nabla_\perp \cdot (2D\rho\vec{P} + \rho\delta\vec{n}) = 0 . \tag{B7}$$

Returning to the path integral for a single polymer (2.1), we identify the Euclidean Lagrangian as

$$L = \frac{1}{4D} \left[\frac{d\vec{r}}{dz} - \delta\vec{n} \right]^2 . \tag{B8}$$

Leading to the Euclidean momentum

$$\vec{p} = i \frac{\partial L}{\partial \dot{r}} = \frac{i}{2D} \left[\frac{d\vec{r}}{dz} - \delta\vec{n} \right] \tag{B9}$$

so that

$$\frac{d\vec{r}}{dz} = 2Di\vec{p} + \delta\vec{n} . \tag{B10}$$

Apparently, $\vec{P}$ is the field associated with $i\vec{p}$. Letting $\vec{v}$ be the field equivalent of the velocity, we have

$$\vec{v} = 2D\vec{P} + \delta\vec{n} , \tag{B11}$$

so our constraint becomes

$$\partial_z \rho + \nabla_\perp \cdot (\rho\vec{v}) = 0 . \tag{B12}$$

Note that $\rho\vec{v} = \vec{t}$ is the "momentum" field of our quantum bosons, which we have called the "tangent" field in the previous sections. We now replace $\vec{P}$ by $(\vec{v} - \delta\vec{n})/2D$ in (B5). Upon expanding ρ around some mean-field value ρ_0, we are lead to the hydrodynamics of Sec. V.

If we were to add sources to the theory, (B1) is changed by

$$\delta S_p = - \int dz\, d^2r\, 2h\sqrt{\rho} \cos\theta . \tag{B13}$$

We may expand this term in powers of θ if the fluctuations in θ are small, which they will be if the polymers are sufficiently long. To lowest order (B13) is

$$\delta S_p = \int dz\, d^2r\, h\sqrt{\rho}\theta^2 \ . \tag{B14}$$

Now upon integrating out θ, we no longer have a δ functional as in (B4), but instead

$$Z = \int \mathcal{D}\vec{v}\,\mathcal{D}\rho\, e^{-S_H} \tag{B15}$$

with

$$S_H = \int dz\, d^2r \left[D\rho(\vec{v}-\delta\vec{n})^2 + \frac{D(\nabla_\perp\rho)^2}{4\rho} - \mu\rho + \frac{v}{2}\rho^2 + \frac{1}{4h\sqrt{\rho}}[\partial_z\rho + \nabla\cdot(\rho\vec{v})]^2 \right] \tag{B16}$$

resulting in the hydrodynamic theory of finite length polymers (5.5). There we had the term

$$\frac{1}{2}\frac{G}{k_BT}(\partial_z\rho + \nabla\cdot\vec{t})^2 \ . \tag{B17}$$

Recalling $G = k_BTl/2\rho_0$ and $l = \rho_0^{-1/2}/h$, we have $\frac{1}{2}(G/k_BT) = (4\sqrt{\rho_0}h)^{-1}$, as required.

The integration over θ in (B3) needs a more careful analysis. Indeed, it will constrain the number of lines passing through a surface to an integer. When changing variables from ψ and ψ^* to ρ and θ, theta is only determined mod 2π. Because of this, we can consider field configurations in θ which increase by 2π as we go around a particular line. This vortex line is analogous to a point vortex in the two-dimensional XY model. We can now consider a closed vortex loop (the three-dimensional analog of a vortex-antivortex pair) where θ jumps from 0 to $2\pi n$ as we traverse a surface with the vortex loop as the boundary (a so-called "branch" disk). Rewriting the θ-dependent part of (B3), we have, for a volume Σ bounded by the surface $\partial\Sigma$,

$$i\int_\Sigma dV(\rho\partial_z\theta + \vec{t}\cdot\nabla_\perp\theta) = i\int_{\delta\Sigma} d\mathbf{S}\cdot\mathbf{T}\theta - i\int_\Sigma dV\,\theta(\partial_z\rho + \nabla_\perp\cdot\vec{t}) \ , \tag{B18}$$

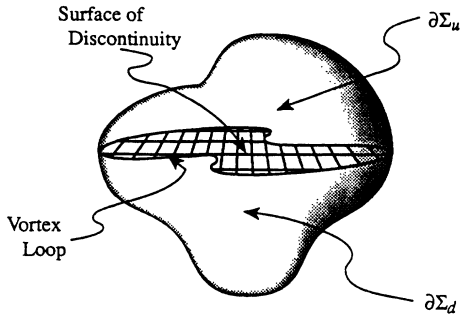

FIG. 16. Surface on which a vortex loop lies. The plane, denoted by hashed lines, is the "branch disk" on which the phase θ jumps discretely by a multiple of 2π.

where $\mathbf{T} = (t_x, t_y, \rho)$ is the three-dimensional particle current. The volume integral on the right-hand side of (B18) will lead to the constraint (B12) in the volume V, when θ is functionally integrated over. The surface integral contains the new constraint.

Consider a vortex line that lies on the surface $\partial\Sigma$ (see Fig. 16). If we now split $\partial\Sigma$ into the parts above and below the surface of discontinuity, $\partial\Sigma_u$ and $\partial\Sigma_d$, respectively, the surface integral is

$$2\pi i n\int_{\delta\Sigma_u} d\mathbf{S}\cdot\mathbf{T} + i\int_{\partial\Sigma} d\mathbf{S}\cdot\mathbf{T}\theta_s \ , \tag{B19}$$

where θ_s is the smoothly varying part of θ. In the same way that we generated the equation of continuity, the second integral will constrain the total flux through the closed surface $\delta\Sigma$ to be 0 (no free ends). However, upon summing over all possible values of n, the first integral in (B19) will constrain the "flux" of lines passing through the surface $\partial\Sigma_u$ to be an *integer*. If polymers are dense and entangled, this set of nonlocal constraints should be unimportant in the hydrodynamic limit, where the fluctuations in θ are small.

*Permanent address: Laboratoire de Physique Theorique de l'Ecole Normale Superieure Paris, 24 rue Lhomond, 75231 Paris CEDEX.

[1] D. R. Nelson, Phys. Rev. Lett. **60**, 1973 (1988); D. R. Nelson and H. S. Seung, Phys. Rev. B **39**, 9153 (1989); D. R. Nelson, J. Stat. Phys. **57**, 511 (1989).

[2] For a review, see D. R. Nelson, in *Proceedings of the Los Alamos Symposium, 1991: Phenomenology and Applications of High Temperature Superconductors,* edited by K. Bedell *et al.* (Wiley, New York, 1992).

[3] A. A. Abrikosov, Zh. Eksp. Teor. Fiz. **32**, 1442 (1957) [Sov. Phys. JETP **5**, 1174 (1957)].

[4] M. C. Marchetti and D. R. Nelson, Phys. Rev. B **41**, 1910 (1990).

[5] A. I. Larkin, Zh. Eksp. Teor, Fiz. **58**, 1466 (1970) [Sov. Phys. JETP **31**, 784 (1970)].

[6] M. P. A. Fisher, Phys. Rev. Lett. **62**, 1415 (1989); D. S. Fisher, M. P. A. Fisher, and D. A. Huse, Phys. Rev. B **43**, 130 (1991); E. M. Chudnovsky, *ibid.* **40**, 11 355 (1989).

[7] S. P. Obukhov and M. Rubinstein, Phys. Rev. Lett. **65**, 1279 (1990).

[8] P. G. De Gennes, in *Polymer Liquid Crystals,* edited by A. Ciferri, W. R. Kringbaum, and R. B. Meyer (Academic, New York, 1982), Chap. 5.

[9] R. B. Meyer, in *Polymer Liquid Crystals* (Ref. [8]), Chap. 6.

[10] T. Odijk, Macromolecules **17**, 2313 (1986).

[11] F. Livolant and Y. Bouligand, J. Phys. (Paris) **47**, 1813 (1986); R. Podgornik, D. C. Rau, and V. A. Parsegian, Macromolecules **22**, 1780 (1989).

[12] H. Block, *Poly(γ-Benzyl-L-Glutamate) and Other Glutamate Acid Containing Polymers* (Gordon and Breach, London, 1983).

[13] R. B. Meyer, F. Lonberg, V. Tarututa, S. Fraden, S. D.

Lee, and A. J. Hurd, Discuss. Faraday Chem. Soc. **79**, 125 (1985).
[14] S. Chandrasekhar, B. K. Sadashiva, and K. A. Suresh, Pramana **9**, 471 (1977).
[15] Nguyen Huu Tinh, H. Gasparoux, and C. Destrade, Mol. Cryst. Liq. Cryst. **68**, 101 (1981); T. K. Attwood, J. E. Lyndon, and F. Jones, Liq. Cryst. **1**, 499 (1986).
[16] S. A. Safran, L. A. Turkevich, and P. Pincus, J. Phys. Lett. (Paris) **45**, L69 (1984).
[17] A. Blumstein, G. Maret, and S. Villasagar, Macromolecules **14**, 1543 (1981).
[18] P. G. de Gennes, C. R. Acad. Sci. Ser. B **281**, 101 (1975).
[19] P. G. de Gennes, Mol. Cryst. Liq. Cryst. (Lett.) **102**, 95 (1984).
[20] A. Blumstein, in *Liquid Crystalline Order in Polymers,* edited by A. Blumstein (Academic, New York, 1978); E. M. Barrall II and J. F. Johnson, J. Macromol. Sci. Rev. Macromol. Chem. C **17**, 137 (1979).
[21] A. Stroobants, H. N. W. Lekkerkerker, and Th. Odijk, Macromolecules **19**, 2232 (1986).
[22] S. Fraden, G. Maret, D. L. D. Caspar, and R. B. Meyer, Phys. Rev. Lett. **63**, 2068 (1989).
[23] R. E. Rosenweig, *Ferrohydrodynamics* (Cambridge University Press, New York, 1985).
[24] T. C. Halsey and W. Toor, Phys. Rev. Lett. **65**, 2820 (1990), and references therein.
[25] X. Ao, X. Wen, and R. B. Meyer, Physica A **176**, 63 (1991).
[26] P. Le Doussal and D. R. Nelson, Europhys. Lett. **15**, 161 (1991).
[27] For a discussion of this transition, see L. Balents, R. D. Kamien, P. Le Doussal, and E. Zaslow, J. Phys. I (Paris) **2**, 263 (1992).
[28] J. Toner, Phys. Rev. Lett. **68**, 1331 (1992).
[29] J. Cardy, J. Phys. A **16**, L355 (1983).
[30] P. G. de Gennes, J. Phys. (Paris) Lett. **36L**, 55 (1975).
[31] J. Selinger and R. Bruinsma, Phys. Rev. A **43**, 2910 (1991).
[32] J. P. Bouchaud and A. Georges, Phys. Rep. **195**, 127 (1990); P. Le Doussal and J. Machta, Phys. Rev. B **40**, 9427 (1989).
[33] D. R. Nelson, in *Phase Transitions and Critical Phenomena,* edited by C. Domb and J. L. Lebowitz (Academic, New York, 1983), Vol. 7, and references therein.
[34] D. R. Nelson and R. A. Pelcovits, Phys. Rev. B **16**, 2191 (1977).
[35] P. Le Doussal (unpublished).
[36] D. R. Nelson and P. Le Doussal, Phys. Rev. B **42**, 10 113 (1990).
[37] J. W. Negele and J. Orland, *Quantum Many-Particle Systems* (Addison-Wesley, New York, 1988), Chaps. 1 and 2.
[38] V. N. Popov, *Functional Integrals and Collective Excitations* (Cambridge University Press, New York, 1987).
[39] J. dex Cloiseaux, J. Phys. (Paris) **36**, 281 (1975); see also R. G. Petschek and P. Pfeuty, Phys. Rev. Lett. **58**, 1096 (1987).
[40] P. G. de Gennes, *Scaling Concepts in Polymer Physics* (Cornell University Press, Ithaca, N. Y. 1970).
[41] M. E. Fisher, Rep. Prog. Phys. **30**, 615 (1967).
[42] L. S. Ornstein and F. Zernike, Proc. Acad. Sci. Amsterdam **17**, 793 (1914).
[43] D. R. Nelson, Physica A **177**, 220 (1991).
[44] J. V. Selinger and R. F. Bruinsma, J. Phys. II (Paris) **2**, 1215 (1992).
[45] As follows, e. g., from the solution of Problem 5-13, in D. A. McQuarrie, *Statistical Mechanics* (Harper and Row, New York, 1976).
[46] V. G. Taratura and R. B. Meyer, Liq. Cryst. **2**, 373 (1987).
[47] J. Toner and D. R. Nelson, Phys. Rev. B **23**, 316 (1981).
[48] D. Forster, D. R. Nelson, and M. J. Stephen, Phys. Rev. A **16**, 732 (1977).
[49] B. I. Halperin, P. C. Hohenberg, and S. K. Ma, Phys. Rev. Lett. **29**, 1548 (1972).
[50] P. G. de Gennes, Phys. Lett. **38A** 339 (1972).
[51] D. J. Bergman and B. I. Halperin, Phys. Rev. B **13**, 2145 (1976).
[52] Terry Hwa (private communication) has produced a similar derivation.

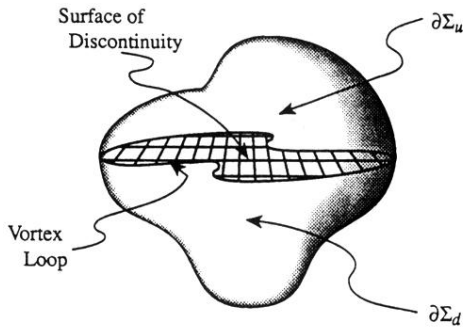

FIG. 16. Surface on which a vortex loop lies. The plane, denoted by hashed lines, is the "branch disk" on which the phase θ jumps discretely by a multiple of 2π.